Atmospheric temperature and public support for climate policy

in a coupled ecological-economic-social model

Marjolein van den Berghe

Atmospheric temperature and public support for climate policy

in a coupled ecological-economic-social model

by

Marjolein van den Berghe

19 June 2026

to obtain the degree of Master of Science in Applied Mathematics

at the Delft University of Technology,

to be defended publicly on Thursday 9 July 2026 at 14:00.

Student number:	5087724		
Date:	19 June 2026		
Thesis committee:	dr. ir. Y. M. Dijkstra,	TU Delft EEMCS,	Mathematical Physics
	dr. G. Marangoni,	TU Delft TPM,	Multi-Actor Systems
	A. Poujon,	TU Delft TPM,	Policy Analysis
	dr. ir. E. G. Rens,	TU Delft EEMCS,	Mathematical Physics

Delft University of Technology

Faculty of Electrical Engineering, Mathematics and Computer Science

Abstract

Current climate policy is not sufficient to reach the Paris agreement [1], where nations agreed that global temperature increase should remain below 2 °C. In this thesis an ecological-economic model (Dynamically Integrated model for Climate and Economy) is coupled to a social model to investigate the effect of this coupling on global warming. In particular, the atmospheric temperature is coupled to the public support for climate policy. In all model simulations, the level of public support rises to full support eventually. The way in which public support evolves to full support seems determinant for a high or low global warming in the model. In the case that public support rises quickly, the global warming stays in the desired limit of 2 °C. However, in the case that public support levels initially fall and eventually tip to full support, the model shows high global warming. In these cases, bifurcation-induced and rate-induced tipping were identified. There are multiple factors that can cause a delay in achieving full support for climate policy or climate policy implementation in general. They are the following: a low value of the perceived weight for the costs of climate change ν_2, a low social learning rate κ and a low maximum bound for the change in climate policy $\Delta_{\mu_{max}}$. The change of one factor can also impact the influence another factor has. An important example of this is the strength of social norms δ; a change in this variable influences the sensitivity of ν_2 and x_0.

Contents

Chapter 1

Introduction

According to the World Meteorological Organization (WMO), the years 2015 till 2025 were the hottest 11 years on record [2]. In 2025, the global average temperature was $1.43 \pm 0.13\ ^{\circ}C$ above the average temperature of 1850-1900. The global mean surface temperature is rising and this change of climate has an effect on extreme climate events [2]. Some examples in the year 2025 are the following: flash flooding that led to hundreds of reported deaths in Africa and thousand in Asia, droughts and wildfires in North and South America and heatwaves in Europe [3].

Attention to climate change has changed over the last century. In the first half of the 20th century, the science community was convinced that climate change only happened on very slow timescales. They were familiar with the changes due to the coming and going of ice ages. However, they believed that these changes happened in multiple thousands of years [4]. In the second half of the century, this belief began to shift as they discovered more anomalies and proofs that Earth's climate could change faster in the span of thousands or hundreds of years. In 1993, two holes were drilled in the Greenland ice plateau 30 kilometres apart from each other. The similarities between the ice cores convinced the scientists that the results of their measurements were not caused by local fluctuations. The scientists concluded from the research that an increase of 7 °C within 50 years had happened in the history of Greenland [4]. The second half of the 20th century was also a time where the role of humans in climate change became more apparent. Previously, this was only a topic of interest for scientists and entrepreneurs, but in the 1980s this became a topic for the intergovernmental agenda together with environmental challenges such as the depletion of the ozone layer [5]. An important milestone in the intergovernmental climate policy was the Paris agreement in 2015, where it was agreed upon to limit the global average temperature under 2 °C, preferably under 1.5 °C [6].

Currently, policies and Nationally Determined Contributions stated by nations are not sufficient to meet this goal [6].

There are numerous studies on climate policy and climate change that investigate how to reach this goal, informing policy makers as well as the public. E.g., William Nordhaus introduced DICE, an optimization model for finding policies that balance climate and economy objectives [7]. A simpler climate model for modelling climate change is the global energy balance model [8]. Global climate models can be so complex and time consuming that they implement neural networks for solving them [9]. Models can also focus on the interaction between ecology and sociology [10], [11]. The first social model is a simple social model with one process modelling public support for climate policy. The second model is more complex with multiple feedback processes for perception of weather, interaction of the public with the government and law and other social dynamics. These models describe the effects of climate policy or the interaction between the public and climate. For the implementation of climate policies, public support is important in democracies [12]. A shift in public opinion can support or oppress climate policy. Public opinion can be subject to tipping; the process where a small change in a system leads to a large, rapid, qualitative shift in the system. When enough people conform to a new social norm, this could result in tipping society to this new norm [13]. Thus public support is a factor in shaping climate policy, however, economy is also an important factor policy makers take into consideration. There is less research on this interaction between public support, ecology and economy. In this thesis we design a model that couples an ecological-economic model with a social model. This model is relatively simple because it contains few equations, but starting with a simple social model can help to develop analysis methods, results and potentially the finding of tipping points. These findings can contribute to the design and research of coupled models with more complex social models.

The goal of this research is to investigate how the coupling between atmospheric temperature and public support influences global warming in a coupled ecological-economic-social model. In particular, an interest of this thesis is the finding of tipping points that influence climate change in a positive or negative way.

For this research, the Dynamic Integrated Climate-Economy model (DICE) version 2023 is coupled with the social model of public support by Maghsoodlo et al. [10]. These models are coupled with various parameters, such as the bounds that the change of climate policy is subjected to (as execution of climate policy can be restricted by for example technical aspects and institutional inertia). Other parameters are the following: the perception of mitigation and damage costs by the public, the strength of the social norms, and the social learning rate for mitigating and non-mitigating behaviour of peers.

This report is structured as follows. In chapter 2 integrated assessment models are introduced as well as research performed with these models. The different definitions of tipping points in multiple research fields are discussed as well. This is followed by a description of the models used in this thesis together with an explanation of the coupling between these models in chapter 3. In chapter 4 the results and equilibria analysis of the separate models are discussed. After this, the results of the coupled model are shown in chapter 5. This is followed by a discussion (chapter 6) and conclusions (chapter 7).

Chapter 2

Theory

In this chapter, we focus on literature regarding Integrated Assessment Models and definitions of tipping points. Section 2.1 introduces integrated assessment models together with their purpose. This is followed by some examples of integrated assessment models and their practical use in section 2.2. As the term tipping point has become popular and widely used in multiple research fields, section 2.3 shows examples of definitions found in literature.

2.1 Integrated Assessment Models

Integrated Assessment Models (IAMs) play a role in the interface between science and policy and are also studied in science. IAMs are used in the context of climate change and the evaluation of policy in relation to this topic. Parson and Fisher-Vanden [14] explain the concept of Integrated Assessment Models (IAMs) and their purposes regarding climate change, mitigation and climate adaptation. The *assessment* part of these models is to encapsulate the knowledge of a specific research field which is then used to inform policy makers. The questions by policy makers can be complex, which makes knowledge from one research field insufficient. To provide answers for these questions, knowledge and expertise from various research fields are combined into an *Integrated* Assessment Model. There are different ways in which an IAM can contribute to science and policy making [14]. Firstly an IAM can be used to project the trajectory of climate change and show how different choices in policy could influence the impact of climate change on the society or economy. Secondly an estimate can be made of the costs for emission mitigation for different scenarios. For example, some models aim to find the optimal mitigation policy with the least damage to the economy while protecting the environment. These estimates are, however, subject to the uncertainties accompanied by modelling the future. Thirdly IAMs can be used to identify and gauge these uncertainties which could initiate further research of the specific model that is linked to the uncertainties. Lastly, one of the purposes of IAMs can be to identify and quantify feedback processes in the system. This can improve the understanding of the system.

2.1.1 Coupling of ecology with economy or sociology

An integral part of an IAM is combining multiple research fields into one model. IAMs investigating climate change can couple ecology and economy or ecology and sociology. This section presents a few brief examples of such couplings.

An example of an IAM that couples economy and ecology is DICE. It links economic growth and investment to CO_2 emissions. These CO_2 emissions result in temperature changes which lead to economic damage. DICE is typically used to investigate when investments in mitigation policies are optimal. Optimal mitigation policies are calculated for different scenarios; for example the prevention of surpassing 2°C threshold. More on DICE later in section 2.2.1 and 3.1.

Current policy of governments is not sufficient to achieve the goal of a maximum warming of 2 °C [1]. This is where coupled socio-ecological models can contribute; these models investigate for example how the social norms can influence policy through the political apparatus [11] or what the effect of actions from society is on the environment and vice-versa [10]. Moore et al [11] investigated multiple feedback processes in a coupled socio-ecological model. As an example, they mention that extreme weather conditions can strengthen individuals in their belief of climate change. This is however also subject to their pre-existing beliefs. Furthermore, the baseline of 'normal' weather is constantly updated with recent weather events. Maghsoodlo et al. [10] study a different socio-ecological model where they divide the population in two social groups: mitigators and non-mitigators. They couple the Earth System Model to equations representing behavioural dynamics and investigate different tipping points with respect to the fraction of people in the social group of mitigators. They found that increasing the social learning rate (the rate at which individuals can learn and switch between groups) would delay or prevent the tipping point of the climate model. A limitation of the behavioural model is the assumption that the two social groups are homogenously mixed among the population.

When designing a coupled IAM, one has to decide which aspects are included in the model. Usually, many of the highly complex processes are represented by simpler variables. These variables can either be imposed on input (exogenous parameter), or computed within the model (endogenous parameter). The choice for imposing variables as endogenous or exogenous variables influences the results of the model. Endogenous variables are influenced by the control variables, whereas exogenous variables are not influenced by the model computations. Pasqualino et al. [15] discuss the choice of including the variable of induced innovation (innovation induced by implementing a technology, specifically leading to lower-cost sustainable economy) as exogenous or endogenous. They state that treating induced innovation endogenously is important, since this encourages policy makers to make decisions that stimulate induced innovation. After studying different models, they produced a decision tree to help policy makers find the best model to answer a specific policy question.

2.2 Examples of Integrated Assessment Models

This section shows some examples of IAMs. An important model in the analysis of climate change policy is DICE. Section 2.2.1 focuses on the DICE model and various critiques on this model. Other IAMs such as IAMs that work with multiple regions (2.2.2) or are agent-based (2.2.3) are discussed as well.

2.2.1 DICE

DICE is developed in 1992 by Nordhaus and is used for projections of emissions and temperature under different economic and social states of the world [16]. DICE is an optimization model with an objective of maximizing social welfare, which is expressed in monetary terms by present and future discounted economic output. Figure 2.1 shows the connections between the different model variables. Economic *output* is increased by *investment*. A portion of this output is reduced by *damage costs* from rising temperatures. Another variable that reduces the output is the *abatement cost* from mitigation of CO_2 emissions. This cost depends on the fraction of emission reduction; the *emission control rate*. The *emission control rate* reduces the CO_2 *emissions* from industry (calculated from *output*) and is the exogenous parameter that is used for the optimization. The *emissions* influence the *temperature* which in their turn influence the *damage cost*. As mentioned before the *damage* and *abatement costs* are subtracted from the *output* of the economy. The remaining output is called *global product* from which a portion is used as *investment* for the future.

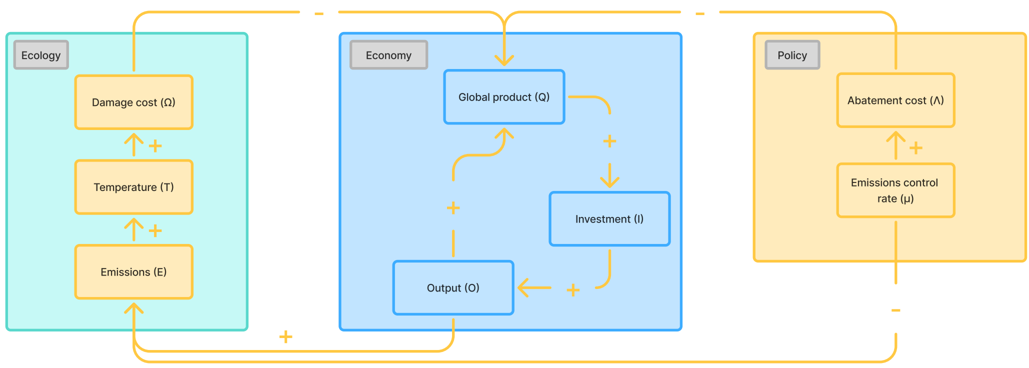

Figure 2.1: A simplified schematic overview of the underlying model equations of DICE. '+' or '−' indicate that an increase in the first variable results in an increase or decrease, respectively, for the second variable.

Critique on DICE

As DICE has been an important model in the field of integrated assessment models for multiple decades there are also critique points. Cai et al. [17] state that the use of different difference methods for the economic and ecological equations (explicit and implicit methods, respectively) could result in errors. They also criticize the choice for the time step, as they question if a continuous-time model such as climate models can be accurately modelled with a time step of a decade. They introduce a continuous-time version of DICE in their paper to show an alternative approach. Another problem they address is the non-physicality of the radiative forcing equation; the amount of CO_2 in 2035 affects the warming between 2015 and 2025. Ikefuji et al. [16] argue that the economic and ecological equations of DICE are unnecessary complicated and could be simplified. This would lend to a more transparent and robust model. They also propose to change the damage function such that extreme risk experiments can be executed with DICE. Grubb et al. [18] criticize the implementation of abatement costs because of the assumed independence; the cost for abatement does not depend on the cost or mitigation in previous time steps.

2.2.2 Multiple regions

Climate change is a challenge for the whole population of the Earth. Every country will have to deal with it to some extent in the future, or is already dealing with it. There is a sentiment that one country can only do so much; that the efforts of one government would not be sufficient. Nations are working together to make agreements and promises. The difficulty in this is that some nations have more resources to prevent or to adapt to climate change. DICE has a version that incorporates multiple regions, called RICE (Regional Integrated of Climate and Economy). Two examples of questions asked in research regarding IAMs for multiple regions are: how much influence can the policy of one nation have and how should mitigation goals be divided across all nations?

An example of a policy is that of carbon pricing. This would ensure that products or services resulting in higher CO_2 emissions become more expensive than sustainable alternatives. It is likely that such a policy would disbenefit the economy of the country that implements this policy as products and services will be bought from other countries. [19] studies the effect of implementing carbon pricing on diffusion of this policy to other countries. They conclude that implementing the policy can inspire other countries and increase their influence on global emissions.

Currently, there is critique on how mitigation goals are divided between nations. Cost benefit IAMs are used for a substantial amount of mitigation pathways developed by the Intergovernmental Panel of Climate Change [1] [21]. A concern with IAMs based in cost benefit optimization is how they lead to an unfair distribution of fossil fuel energy use per capita for developed nations and put a damper on the possible growth of developing nations [22]. In this way vulnerable nations that have a very small contribution to global warming face economic inequality. Combine this with the ecological impacts they would face, they would not have the resources to adapt to the rapid changes of the climate. Biswas et al. [21] explore other mitigation paths in different ethical frameworks to find pathways that encourage climate justice. The authors of this paper developed the JUSTICE model that couples the RICE50+ model (i.e. RICE model with more than 50 regions) with the FaIR climate model. They optimize four objectives; maximize overall well-being, minimize economic loss due to climate damages, reduce mitigation costs and limiting the number of years the 2 °C threshold is passed. In their research four different general social welfare functions are compared, each one related to a different ethical framework.

2.2.3 Agent-based modelling

A different approach to IAMs is that of agent-based modelling. In agent-based modelling, the model consists of multiple actors (agents) that interact with the modelled environment and/or each other [23]. Agent-based modelling can provide a tool to study social or complex systems. The model of

[1] The Intergovernmental Panel of Climate Change (IPCC) is a body of the United Nations that analyzes scientific outcomes regarding climate change to inform policy makers [20].

Lamperti et al. [24] simulates climate damages and how these differ on microscopic and macroscopic scale. The conclusion is that the damages in the ABM are significantly larger than in other more general IAMs.

2.3 Definitions of tipping points

In general, tipping points can be thought as fast, qualitative changes in a system that are not (easily) reversible. The first reference of tipping point is with respect to racial segregation [25], later the term became popular with the book 'tipping point' of Gladwell [25]. The term is currently used in multiple scientific fields. This section discuses several definitions of the term tipping point found in literature.

A complicating point with the frequent use of tipping point, is that the definition across scientific fields is not consistent [26]. Milkoreit et al. [26] performed a literature study with a quantitative and qualitative analysis on the use and meaning of tipping points in multiple research fields. Gathering the results of the analysis, the authors propose the following initial definition for tipping points:

"[...] tipping points in general can be defined as the point or threshold at which small quantitative changes in the system trigger a non-linear change process that is driven by system-internal feedback mechanisms and inevitably leads to a qualitatively different state of the system, which is often irreversible. This new state can be distinguished from the original by its fundamentally altered (positive and negative) state-stabilizing feedbacks." [26], p. 9

In this definition there are four conditions stated that make something a tipping point: 1) multiple stable states, 2) a rapid change, 3) feedback processes as system-internal mechanisms and 4) a weakened irreversibility. With weakened they mean that hysteresis is allowed or that the process is irreversible on timescales relevant to human societies. Milkoreit et al. [26] argue that more research is needed in order to extend this definition to social tipping points and examine potential differences between tipping points in ecological and social systems. Even in the case that these tipping points are similar, the research field of social systems could face methodological challenges in examining social tipping points.

In the field of mathematics, tipping describes the event of switching between branches of equilibrium solutions. It is possible in an autonomous system for there to be multiple branches of equilibrium solutions with respect to some parameter λ. When this autonomous system is shifted to a non-autonomous system where λ changes in time, tipping can occur. There is a proposition that tipping phenomena can be divided mathematically in three distinct categories; bifurcation-induced tipping, noise-induced tipping and rate-induced tipping [27], [28].

The first category is that of bifurcation-induced tipping. Consider a system of equations **f**, with **y** representing the state of the system and some parameter λ. Assume that this system has multiple branches of equilibrium solutions. A mathematical definition of a bifurcation point for such a system is given by Seydel [29]; a bifurcation (with respect to parameter λ) is a solution $(\mathbf{y}_0, \lambda_0)$ of system

$$0 = \mathbf{f}(\mathbf{y}, \lambda), \tag{2.1}$$

where the number of solutions changes in the case that λ passes through this solution. An example of such a bifurcation is shown in the bifurcation diagram of Figure 2.2. At λ_0, the system changes from having one to three possible solutions. At λ_1, the system shifts again but this time from three to one possible solution. At these two points there is a fold bifurcation in the system. If the non-autonomous system is close to the lower branch at some point between λ_0 and λ_1 and λ would increase, the system will follow the branch until the bifurcation point where the branch is no longer stable. If λ increases further the system will converge to the upper branch. This tipping phenomenon between two stable branches is called bifurcation-induced tipping and sketched in Figure 2.2 a).

The second category for tipping in the field of mathematics is that of noise-induced tipping. This happens when the system is perturbed which leads to the system converging to a different stable state. In Figure 2.2, this could happen when the system is between λ_0 and λ_1, close to the lower branch and **y** is perturbed significantly. If this perturbation causes **y** to cross the unstable solution, the closest attractor is the upper branch to which the system will converge. This switching between branches due to a perturbation is called noise-induced tipping and sketched in Figure 2.2 b). The difference between bifurcation-induced tipping and noise-induced tipping with respect to perturbations and recovery is further explained in Figure 2.3.

The last category is that of rate-induced tipping. Here the parameter of interest is changing at a specific rate. Assume that the system is not yet at a stable branch. For example, in Figure 2.2 c), the system could be to the left of the two folds. If the rate at which parameter λ changes is slow (solid orange line), the system has time to converge to the lower stable branch. On the other hand, if the rate is very large (dashed $(- \cdot \cdot -)$ purple line), the system crosses the unstable equilibrium

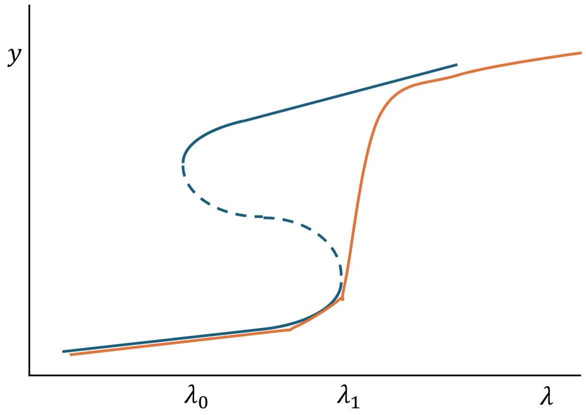

(a) Bifurcation-induced tipping

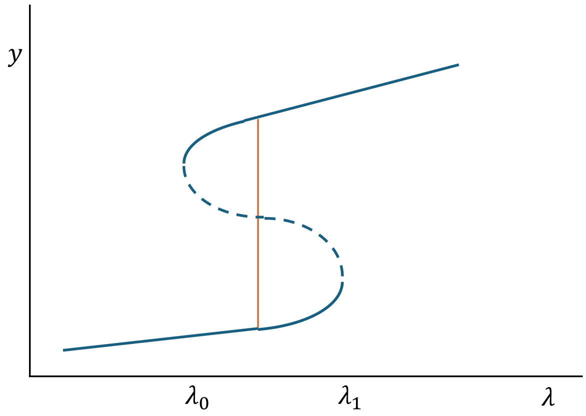

(b) Noise-induced tipping

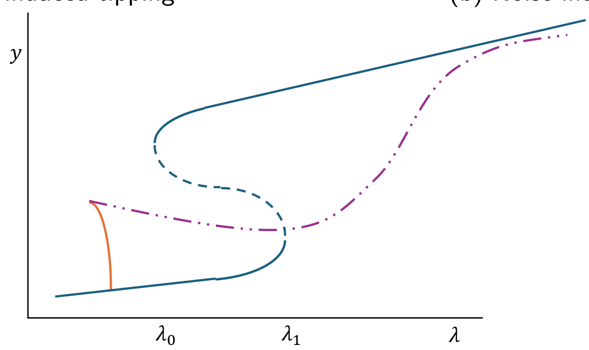

(c) Rate-induced tipping, where the solid orange line represents a fast rate and the purple dashed (— · · —) line a slow rate.

Figure 2.2: Example of a fold bifurcation in some model with variable y and parameter λ. The blue lines are solutions of the autonomous system with solid lines for stable and dashed lines for unstable solutions. Three tipping phenomena are sketched in orange and purple.

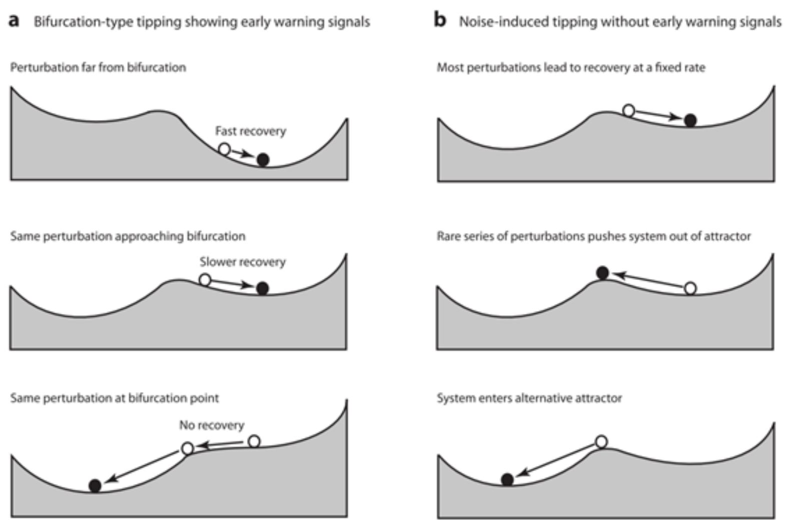

Figure 2.3: The difference between bifurcation- and noise-induced tipping in relation to perturbations and their recovery. Stable attractors are represented with valleys and the state of the system with a ball. [28]

(dashed blue line) and is attracted to the higher branch. This difference in rate changes the attractor to which the state converges and is called rate-induced tipping.

Milkoreit et al. [26] found that in the field of social-ecological systems the term tipping point is also used as a replacement for regime shift. They define a regime shift as "a large, persistent change in structure and function of social-ecological systems" [26], p.3. A technical point they mention in relation to this replacement is that a regime shift denotes the process of passing a tipping point. In sociology, synonyms for tipping points are threshold and punctuated equilibrium.

Chapter 3

Model

The models and their adaptations used for the model in this research are discussed in this chapter. The model equations of DICE together with some adaptations are explained in section 3.1. The model used for the social dynamics is introduced in section 3.2 and the coupling between the two discussed models is described in section 3.3.

3.1 DICE

Throughout the years, Nordhaus has adapted the DICE model, resulting in multiple versions. For this thesis the most recent version is used (DICE-2023 [30], [31]) to ensure that the model parameters are calibrated with the latest data. DICE is an optimization model; an objective function represents the desirability of a certain state of the world. In this study the focus lays on a mathematical analysis of the model equations and therefore the objective function is not taken into account. The model equations are used for modelling and projecting future trajectories of climate and economy. We start with explaining the main equations of the DICE-2023 model in section 3.1.1. More details on the parameter values and exogenous parameters formulations can be found in appendix A. The implementation for this thesis project is verified with the code of Ivo Welch in section 3.1.2. The control parameters of DICE are subject to the optimization of DICE. As a consequence of opting out of the optimization, the control parameters need to be defined. The choices for the control parameters are stated and explained in section 3.1.3. We would like to find equilibrium points for the purpose of studying tipping behaviour. It appears that the system of equations needs to be modified in order to find equilibria. These modifications are presented in section 3.1.4.

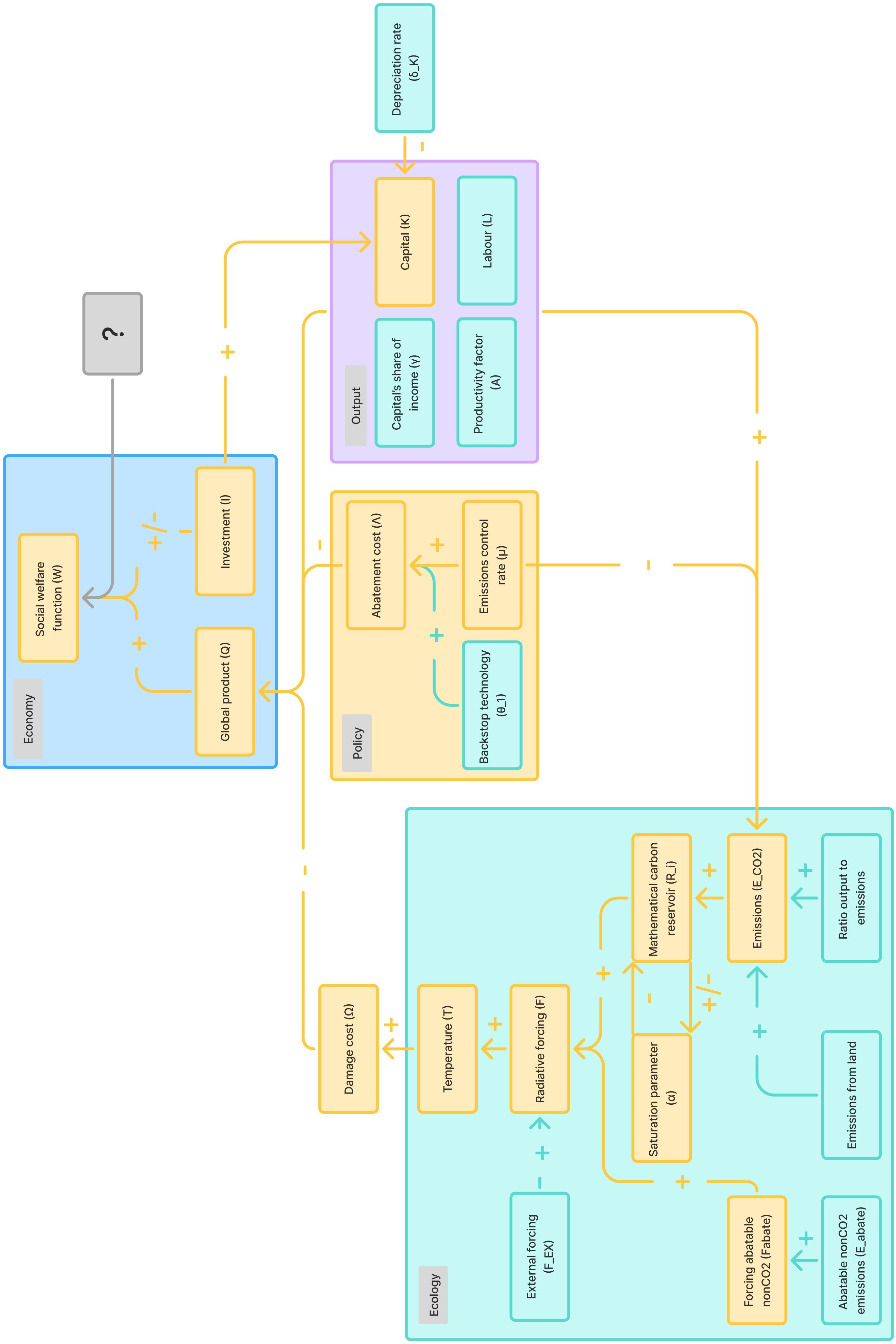

Figure 3.1: Schematic overview of DICE-2023. The endogenous variables are denoted with yellow boxes and the exogenous variables and parameters with turquoise. '+' or '−' indicate that an increase in the first variable results in an increase or decrease, respectively, for the second variable.

3.1.1 DICE-2023 model equations

The model equations of DICE can be divided in three categories: economy, policy and climate. The model equations for each category are shown below. A schematic overview of DICE-2023 is shown in Figure 3.1 and can be used as a reference for the relation between the model variables described in this section.

3.1.1.1 Economy equations

The output of the economy is calculated with the Cobb-Douglas production function, a common equation in macroeconomics [32].

$$O[t_i] = A[t_i]K[t_i]^{\gamma}L[t_i]^{1-\gamma} \tag{3.1}$$

Here, A is the technical efficiency and L is labour. K is physical capital, meaning the value of the machines and other tools needed during production. γ is the elasticity constant representing how income is divided between capital and labour.

Capital loses value in time due to the depreciation rate δ_k but grows due to the adding of investment I, this is shown in the following equation,

$$K[t_i] = I[t_i] - \delta_K K[t_{i-1}]. \tag{3.2}$$

Climate change and climate policy reduce the output of the economy due to damage costs Ω and abatement costs Λ. The gross product Q is what is left after these reductions.

$$Q[t_i] = [1 - \Lambda[t_i] - \Omega[t_i]]O[t_i] \tag{3.3}$$

From Equation (3.3) one can see that Λ and Ω are ratios and not a monetary measure. The equations for Λ and Ω are given in Equations (3.5) and (3.18). In DICE, investment I is linked to gross product Q via the savings rate r; a control parameter determined in the optimization process.

$$I[t_i] = rQ[t_i] \tag{3.4}$$

3.1.1.2 Policy equations

The economy causes carbon emissions, with policy it is possible to abate these emissions. A control parameter of the model tunes which fraction of emissions is reduced. This emission control parameter μ is 1 if all emissions are reduced and 0 if no action with respect to emissions is taken. The corresponding equation for the calculation of fractional abatement costs (Λ) is given by,

$$\Lambda[t_i] = \theta_1[t_i]\mu[t_i]^{\theta_2}, \tag{3.5}$$

where θ_1 is the backstop technology and θ_2 a parameter.

3.1.1.3 Climate equations

The climate changes due to greenhouse gas emissions. In this section we learn about the equations in DICE that represent these processes, starting with the equation for CO_2 from industry and land.

$$E_{CO_2}[t_i] = (\sigma[t_i]O[t_i] + E_{land}[t_i])\,[1 - \mu[t_i]], \tag{3.6}$$

$\sigma(t)$ is the ratio of uncontrolled carbon emissions per economic output and E_{land} the emissions from land-use and deforestation.

These emissions lead to an increase in the atmospheric carbon reservoir. This is modelled by DFAIR [30], a DICE adaptation of the FAIR model. The DFAIR model works with 4 mathematical carbon reservoirs R_j, with no further physical meaning.

$$\Delta R_j[t_{i+1}] = \xi_j E_{CO_2}[t_i] - \frac{R_j[t_i]}{\alpha[t_i]\tau_j}. \qquad j = 1, 2, 3, 4 \tag{3.7}$$

ξ_j is the fraction of emissions going in reservoir j, τ_j the corresponding time constant and α a saturation parameter. In the implementation of Ivo Welch [33] and DICE-2023 [34] another expression for $R_j(t_{i+1})$ was used,

$$R^j[t_{i+1}] = \xi_j E_{CO_2}[t_{i+1}]\tau_j\alpha[t_{i+1}]\left(1 - e^{-\frac{t_i - t_0}{\tau_j\alpha[t_{i+1}]}}\right) + R_j[t_i]e^{-\frac{t_i - t_0}{\tau_j\alpha[t_{i+1}]}}. \tag{3.8}$$

A possible reason for this adaptation is to increase numerical stability. A derivation of Equation (3.8) from Equation (3.7) is included in Appendix B.1. The atmospheric concentrations of carbon

M_{AT} follow from these mathematical reservoirs R_j,

$$M_{AT}[t_i] - M_{AT}[1765] = \sum_{j=1}^{4} R_j[t_i]. \tag{3.9}$$

The accumulated carbon in ocean and land C_{acc} is then found in the following way,

$$C_{acc}[t_i] = \sum_{v=1765}^{t_i} E_{CO_2}[v] - (M_{AT}[t_i] - M_{AT}[1765]). \tag{3.10}$$

The last two equations of the DFAIR model have the purpose to implicitly define saturation parameter α,

$$\text{iRF100}[t_i] = \zeta_0 + \zeta_C C_{acc}[t_i] + \zeta_T T_{AT}[t_i] \tag{3.11}$$

$$\text{iRF100}[t_i] = \sum_{j=1}^{4} \alpha[t_i]\xi_j\tau_j \left(1 - e^{-\frac{100}{\alpha[t_i]\tau_j}}\right). \tag{3.12}$$

We continue with the non-CO_2 greenhouse gases. In version of DICE-2023 the emissions of greenhouse gases that are not CO_2, are split in two categories; abatable and non-abatable. The abatable non-CO_2 emission E_{abate} is an external parameter.

Radiative forcing is the effect that greenhouse gases have on the radiation balance of the Earth [35]. The radiative forcing associated with the abatable non-CO_2 gases F_{abate} is a recursive function.

$$F_{abate}[t_{i+1}] = 0.00955 F_{abate}[t_i] + 0.861 E_{abate}[t_i](1 - \mu[t_i]) \tag{3.13}$$

The radiative forcing from the non-abatable greenhouse gases that are not CO_2 is given by the external parameter F_{EX}. Total radiative forcing follows from adding the different radiative forcing variables and using the atmospheric carbon concentration.

$$F[t_i] = \eta \log_2 \left(\frac{M_{AT}[t_i]}{M_{AT}[1765]}\right) + F_{abate}[t_i] + F_{EX}[t_i], \tag{3.14}$$

with η a radiative forcing parameter.

The atmospheric temperature is calculated recursively with a two-box model from the total radiative forcing $F(t)$. T_1 and T_2 are the temperature differences due to processes of the deep and upper ocean, respectively.

$$T_1[t_{i+1}] = T_1[t_i]e^{-\frac{5}{236}} + 0.324F[t_{i+1}]\left(1 - e^{-\frac{5}{236}}\right) \tag{3.15}$$

$$T_2[t_{i+1}] = T_2[t_i]e^{-\frac{5}{4.07}} + 0.44F[t_{i+1}]\left(1 - e^{-\frac{5}{4.07}}\right) \tag{3.16}$$

$$T_{AT}[t_i] = T_1[t_i] + T_2[t_i] \tag{3.17}$$

The last equation is the damage function. Rising temperatures increase the chance of natural disasters or effect the economy in another negative way.

$$\Omega[t_i] = \psi_1 T_{AT}[t_i] + \psi_2 [T_{AT}[t_i]]^2. \tag{3.18}$$

with ψ_1 and ψ_2 some non-negative parameters.

3.1.2 Verification

The implemented code was tested against the implementation of Ivo Welch. He implemented DICE-2023 in python to make it more accessible for the public [33]. DICE is an optimization program with control variables emission control rate μ and saving rate r. Welch optimized for different scenarios. To verify the code developed for this thesis, the control variables optimized in a specific scenario are given as input. In this case the scenario 'C/B optimal' was used; where the cost-benefits are optimized without other restrictions (temperature constraints for instance). The values of variables are compared with the values of Welchs code. The following function was used:

$$\text{relative error} = \max_i \left(\frac{y_W[i] - y[i]}{y_W[i] + \epsilon} \right) \tag{3.19}$$

With y_W the value of the variable from Welchs code and y the value from this work. $\epsilon = 10^{-6}$ was added to prevent division by (near-)zero. The results are shown in Table 3.1. The relative errors for all the analysed variables are small. The error for emissions is relatively larger, probably because the value goes to zero resulting in a division with almost zero.

Table 3.1: Maximum relative error of different variables between the implementation of Ivo Welch and my own implementation.

Variable		Relative error [-]
Investment	I	$1.66 \cdot 10^{-14}$
Capital	K	$1.73 \cdot 10^{-14}$
Output	O	$4.44 \cdot 10^{-15}$
Emissions CO_2	E_{CO_2}	$6.13 \cdot 10^{-08}$
Carbon concentration in atmosphere	M_{AT}	$2.34 \cdot 10^{-13}$
Abatable forcings	F_{aba}	$1.90 \cdot 10^{-14}$
Total forcings	F	$6.56 \cdot 10^{-11}$
Atmospheric temperature	T_{AT}	$1.04 \cdot 10^{-12}$
Damage cost	Ω	$2.06 \cdot 10^{-12}$
Gross product	Q	$1.71 \cdot 10^{-14}$

3.1.3 Choosing control parameters

3.1.3.1 Savings rate r

One of the control parameters of DICE-2023 is the saving rate r, this parameter is time-dependent. This parameter is not a part of the coupling between public support for climate policy and atmospheric temperature. For this reason we do not investigate the influence of the evolution of saving rate r on the model progression in this thesis. In Figure 3.2 the results of DICE-2023 for r are given for different scenarios where DICE-2023 is used. For all the different scenarios the saving rate becomes constant from around 2220 at the value of 0.28. In most scenarios the saving rate is around this value for the years until 2220. Therefore, for the rest of this thesis we take $r = 0.28$ constant.

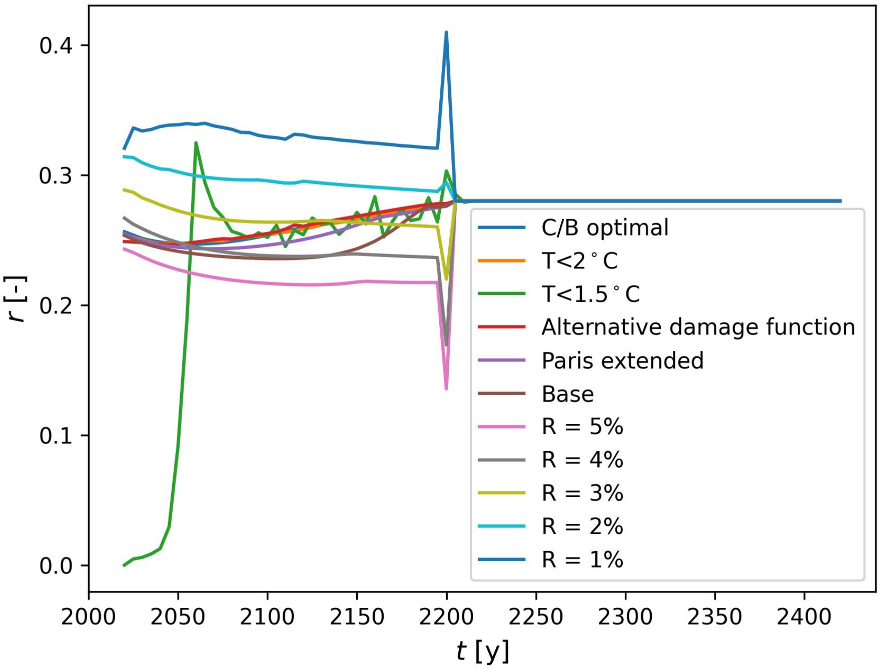

Figure 3.2: The savings rate r that determines what fraction of gross output is used for investment in different scenarios optimized by DICE-2023 (implementation of Ivo Welch [33]) plotted against time. R is the discount rate, the rate at which future consumption is less satisfactory with respect to current consumption.

3.1.3.2 Emissions control parameter μ

We are interested in learning more about the relation between the behaviour of the emissions control parameter μ and the model equilibria. For this purpose we introduce a function for μ. In order to keep the analysis straightforward, only one parameter for the evolution of μ is changed. This will be the time needed for μ to go from the initial value μ_0 to 1, denoted by t_μ. We investigate with two profiles for μ from time 0 to t_μ; a linear profile and that of a hyperbolic tangent. After time t_μ, μ will be 1. The equation for the linear profile is given in Equation (3.20).

$$\mu(t) = \begin{cases} \frac{1-\mu_0}{t_\mu}\, t + \mu_0, & t \leq t_\mu \\ 1, & t \geq t_\mu \end{cases} \tag{3.20}$$

For the hyperbolic tangent a general form is proposed in Equation (3.21). There are two conditions to be fulfilled; $\mu(0) = \mu_0$ and $\mu(t_\mu) = 0.99627$. As $\tanh$ is 1 only in the limit, a value close to 1 was chosen for the second condition.

$$\mu(t) = \frac{1}{2} \tanh\left(\frac{t-a}{b}\right) + \frac{1}{2} \tag{3.21}$$

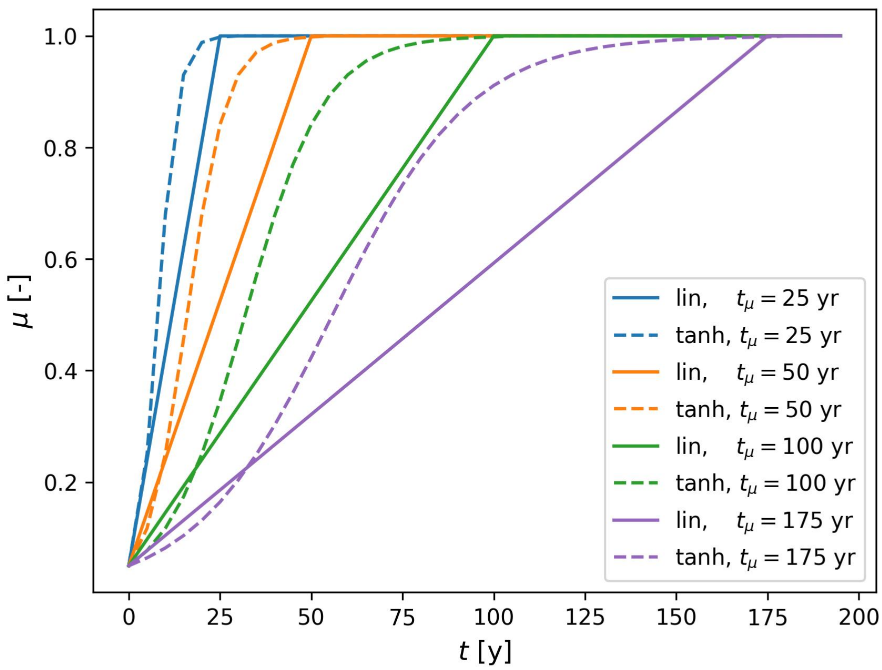

Figure 3.3: Different functions for emissions control parameter μ with a linear (solid) or hyperbolic tangent (dashed) profile for different values of t_μ -time needed for μ to become 1.

The first condition leads to,

$$\begin{aligned}\frac{1}{2}\tanh\left(\frac{-a}{b}\right)+\frac{1}{2}=\mu_0\\ a=-b\tanh^{-1}(2\mu_0-1).\end{aligned} \tag{3.22}$$

This result combined with the second condition leads to,

$$\begin{aligned}0.99627&=\frac{1}{2}\tanh\left(\frac{t_\mu+b\tanh^{-1}(2\mu_0-1)}{b}\right)+\frac{1}{2}\\ 0.99627&=\tanh\left(\frac{t_\mu+b\tanh^{-1}(2\mu_0-1)}{b}\right)\\ \pi&=\frac{t_\mu+b\tanh^{-1}(2\mu_0-1)}{b}\\ b&=\frac{t_\mu}{\pi-\tanh^{-1}(2\mu_0-1)}.\end{aligned} \tag{3.23}$$

The various functions for μ are plotted in Figure 3.3. The area under the curve of μ determines how much mitigation of carbon emissions is implemented in climate policy. The figure shows that the area under the curve for small t_μ is larger. Furthermore, the area under the curve is larger for the hyperbolic tangent function than for the linear function.

3.1.4 System of equations for finding equilibria

At equilibrium, variables do not change over time. For the model equations of DICE this would imply that economic variables such as capital K are constant. However, in macroeconomic models, economy is assumed to always be growing. Stating that the economy can no longer grow, could result in undesirable equilibria. In section 3.1.4.1 we investigate how the model equations will change in the search for equilibria. We learn that a different notion of equilibria is needed in order to find physical meaningful equilibria. For this purpose we use the 2-timescale method. The derivation of the new model with the 2-timescale method can be found in section 3.1.4.2.

3.1.4.1 System for one timescale

We show that an equilibrium implies the absence of carbon emissions. We start with investigating an equilibrium for the difference equation for carbon reservoirs (Eq. (3.7)), repeated below,

$$\Delta R_j[t_{i+1}] = \xi_j E_{CO_2}[t_i] - \frac{R_j[t_i]}{\alpha[t_i]\tau_j}. \qquad j = 1, 2, 3, 4$$

An equilibrium can be found if the emissions every year are in balance with the dissipation of carbon from the reservoirs. As R_j should be constant, a possibility is that changes in E_{CO_2} and α balance each other out. For this to happen, an increase in E_{CO_2} should be accompanied by a decrease in α. However, it appears that the two variables have a positive correlation (more explanation can be found in appendix B.2). Another possibility is that the emissions E_{CO_2} and saturation α are constant. If the constant value of E_{CO_2} is nonzero, the value of C_{acc} keeps changing in time and results in α not being constant. The equations for C_{acc} and α are described in Equations (3.10)-(3.12). From this we conclude that an equilibrium can only be found if the CO_2 emissions become zero.

As can be seen from Equation (3.6), no carbon emissions are only possible when the output from the economy O becomes 0 or the emission control rate μ is 1; as the emissions from land go to 0 for large t. We are not interested in researching the former scenario further. The latter ($\mu = 1$) results in a discoupling of the economy equations; without carbon emissions the economy does not have an influence on the evolution of the ecology. Because of this discoupling, we are only interested in a steady state solution of the climate model. We evaluate multiple exogenous time-dependent parameters in their limit.

$$\lim_{t_i \to \infty} F_{abate}[t_i] = 0 \tag{3.24}$$

$$\lim_{t_i \to \infty} F_{EX}[t_i] = F_{EX} \tag{3.25}$$

In the time domain we are investigating, the accumulation of carbon emission is constant, as a result of the absence of carbon emissions.

$$\lim_{t_i \to \infty} \sum_{v=1765}^{t_i} E(v) = C_{tot} \tag{3.26}$$

Substituting zero CO_2 emissions, the limit of the exogenous parameters and rewriting the equations for T_1 and T_2, the following set of equations are derived for evaluating this climate equilibrium:

$$\begin{cases} \Delta R_j[t_i] & = -\frac{R_j[t_i]}{\alpha[t_i]\tau_j} \qquad\qquad j = 1,2,3,4 \\ 0 & = \sum_{j=1}^{4} R_j[t_i] - (M_{AT}[t_i] - M_{AT}[1765]) \\ 0 & = -C_{acc}[t_i] + C_{tot} - (M_{AT}[t_i] - M_{AT}[1765]) \\ 0 & = -(\zeta_0 + \zeta_C C_{acc}[t_i] + \zeta_T T_{AT}[t_i]) + \sum_{j=1}^{4} \alpha[t_i]\xi_j\tau_j \left(1 - e^{-\frac{100}{\alpha[t_i]\tau_j}}\right) \\ 0 & = -F[t_i] + \eta \log_2\left(\frac{M_{AT}[t_i]}{M_{AT}[1765]}\right) + F_{EX} \\ \Delta T_1[t_i] & = T_1[t_i]\left(e^{-\frac{5}{236}} - 1\right) + 0.324\ F[t_i]\left(1 - e^{-\frac{5}{236}}\right) \\ \Delta T_2[t_i] & = T_2[t_i]\left(e^{-\frac{5}{4.07}} - 1\right) + 0.44\ F[t_i]\left(1 - e^{-\frac{5}{4.07}}\right) \\ 0 & = -T_{AT}[t_i] + T_1[t_i] + T_2[t_i] \end{cases} \tag{3.27}$$

3.1.4.2 System for the 2-timescale method

The system of equations we are studying has fast and slow moving components. For example, the carbon reservoirs R_1 and R_2 restore on timescales of centuries or more, whereas reservoirs R_3 and R_4 restore in decades. While the method of the previous section finds a climate equilibrium for both timescales, it is shown in chapter 4 that the equilibrium of the fast components is more relevant. In this section we derive a new system of equations for finding the equilibrium for fast timescales with the 2-timescale method.

Before the 2-timescale method is applied to the system of equations, the equations from DICE are rewritten. Currently, the DICE equations are maps. For the 2-timescale method it is easier to work with differential equations.

$$R_j[t_i+1] - R_j[t_i] = -\frac{R_j[t_i]}{\alpha[t_i]\tau_j} \qquad j = 1,2,3,4 \tag{3.28}$$

Divide by the timestep $\Delta t = 1$ yr,

$$\frac{R_j[t_{i+1}] - R_j[t_i]}{\Delta t} = -\frac{R_j[t_i]}{\alpha[t_i]\tau_j\Delta t}. \qquad j = 1,2,3,4 \tag{3.29}$$

The conversion from map to differential equation for T_1 and T_2 happen in a similar way.

In DICE the timestep is already included in the variable for decay time; $\tilde{\tau}_j = \tau_j \Delta t$. Substituting this expression and taking the limit $\Delta t \to 0$ yields,

$$\frac{dR_j(t)}{dt} = -\frac{R_j(t)}{\alpha(t)\tilde{\tau}_j}. \qquad j = 1,2,3,4 \tag{3.30}$$

In future notation $\tilde{\tau}_j$ is replaced with τ_j.

For this purpose two new timescales t and τ are introduced to replace the original timescale $\hat{t}$. The variable t represents the fast moving time and τ the slow moving time.

To find this new system of equations we substitute R_j with an order expansion for the first equation,

$$R_j(t,\tau) \approx R_j^0(t,\tau) + R_j^1(t,\tau) + R_j^2(t,\tau) + \dots, \tag{3.31}$$

where the term $\frac{R_j^j}{R_j^0}$ has order $\mathcal{O}(\epsilon^j)$, with the constant $\epsilon = 0.005$ yr^{-1}.

If we take $t = \hat{t}$ and $\tau = \epsilon\hat{t}$, the derivatives with the new timescales become,

$$\frac{\partial R_j}{\partial \hat{t}} = \frac{\partial R_j}{\partial t} + \epsilon\frac{\partial R_j}{\partial \tau}. \tag{3.32}$$

Substitution in the differential equation for carbon reservoirs R_j yields,

$$\frac{\partial R_j^0}{\partial t} + \epsilon\frac{\partial R_j^0}{\partial \tau} + \frac{\partial R_j^1}{\partial t} + \epsilon\frac{\partial R_j^1}{\partial \tau} + \dots = -\frac{1}{\alpha(t,\tau)\tau_i\Delta t}\left(R_j^0 + R_j^1 + \dots\right). \tag{3.33}$$

We classify $\frac{1}{\tau_i}$ as $\mathcal{O}(\epsilon)$ for $i = 1,2$ and $\mathcal{O}(1)$ for $i = 3,4$.

The leading equation of $\mathcal{O}(1)$ for Equation (3.33) is,

$$\begin{cases} \frac{\partial R_j^0}{\partial t}(t,\tau) = 0, & \text{for } i = 1,2 \\ \frac{\partial R_j^0}{\partial t}(t,\tau) = -\frac{1}{\alpha(t,\tau)\tau_i \Delta t} R_j^0, & \text{for } i = 3,4. \end{cases} \tag{3.34}$$

The derivation of the other climate equations are included in appendix B.3.

In conclusion, we have found the new system of equations with the 2-timescale method. There are some significant differences with respect to the previous system of equations; the values of the first two carbon reservoirs (R_1^0 and R_2^0) are constant as well as the influence of processes in the deep ocean on the temperature, T_1.

$$\begin{cases} \frac{\partial R_j^0}{\partial t}(t,\tau) & = 0, \qquad\qquad\qquad\qquad \text{for } i = 1,2 \\ \frac{\partial R_j^0}{\partial t}(t,\tau) & = -\frac{1}{\alpha(t,\tau)\tau_i \Delta t} R_j^0(\tau), \qquad \text{for } i = 3,4 \\ \frac{\partial T_1^0}{\partial t}(t,\tau) & = 0 \\ \frac{\partial T_2^0}{\partial t}(t,\tau) & = T_2^0(t,\tau)\frac{1}{\Delta t}\left(e^{-\Delta t/4.07} - 1\right) + 0.44 F^0(\tau)\frac{1}{\Delta t}\left(1 - e^{-\Delta t/4.07}\right) \\ 0 & = R_1^0(\tau) + R_2^0(\tau) + R_3^0(\tau) + R_4^0(\tau) - M_{AT}^0(\tau) + M_{AT}(1765) \\ 0 & = -C_{acc}^0(\tau) + C_{tot} - (M_{AT}^0(\tau) - M_{AT}(1765)) \\ 0 & = -F^0(\tau) + F_{EX} + \eta \log_2\left(\frac{M_{AT}^0(\tau)}{M_{AT}(1765)}\right) \\ 0 & = -T_{AT}^0(\tau) + T_1^0(\tau) + T_2^0(\tau) \\ 0 & = -(\zeta_0 + \zeta_C C_{acc}^0(\tau) + \zeta_T T_{AT}^0(\tau)) + \sum_{i=1}^3 \alpha^0(\tau)\xi_i\tau_i\left(1 - e^{-\frac{100}{\alpha^0(\tau)\tau_i}}\right) + \alpha^0(\tau)\xi_4\tau_4 \end{cases} \tag{3.35}$$

3.2 Social dynamics

In this section we discuss the behaviour model from Maghsoodlo et al. [10]. The model describes the dynamics of support for climate policy by dividing the population in two groups: mitigators and non-mitigators. Mitigators support climate policy and are willing to pay the costs associated with this, whereas non-mitigators are opposed to climate policy. The model is based on the process of social learning, as described by Bury et al. [36]. With social learning rate κ, a person A samples other people and analyzes their behaviour. In the case that the behaviour of person B is more beneficial, person A switches their behaviour with a probability proportional to the increased benefits. The model equation for the behaviour model [10] is given by,

$$\frac{dx}{dt} = \kappa x(1-x)(-\beta + f(T) + \delta(2x-1)). \tag{3.36}$$

x is the fraction of mitigators (as opposed to non-mitigators) and κ is the social learning rate (yr^{-1}). β the net mitigation cost (-) i.e., the cost for mitigation (for example the purchase of solar panels) minus the savings of mitigation (decreased costs of the energy bill). An important influence on social behaviour are social norms, they can slow down or speed up the switching of behaviours. In this model δ represents the strength of the social norms (-). $f(T)$ is the warming cost function (-) describing the associated costs of climate warming and is defined by,

$$f(T) = \frac{f_{max}}{1 + e^{-\omega(T - T_{lim})}}. \tag{3.37}$$

f_{max} is the maximum cost, T_{lim} is the critical temperature and ω the degree of non-linearity.

3.3 Coupling of the models

The adapted DICE model and social model are coupled with a two-way coupling. Firstly the fraction of mitigators x is coupled to the emission control parameter μ, representing the influence of support levels on climate policy. Secondly the costs of mitigation and damages associated with climate change are used as input for the net mitigation cost β and warming costs $f(T)$. A schematic overview is given in Figure 3.4

The first coupling is represented by the differential equation for μ,

$$\frac{d\mu}{dt}(t) = \Delta\mu_{min}(1-x) + \Delta\mu_{max}x. \tag{3.38}$$

The change in μ is bounded by the parameters $\Delta\mu_{min}$ and $\Delta\mu_{max}$. The change in μ is bounded from above to represent the technical feasibility to mitigate from carbon emissions and is typically 0.04 per year. The lower bound is a representation for the limited sources of fossil fuels; even with full support for the use of fossil fuels, the industry will need to change their energy sources eventually.

The mitigation costs Λ and damage costs Ω from DICE are fractions of the gross product of the global economy and therefore dimensionless. The mitigation cost β and warming cost $f(T)$ of the social model are dimensionless as well. However, they are in a different range; $[0, 2]$ and $[0, 5]$

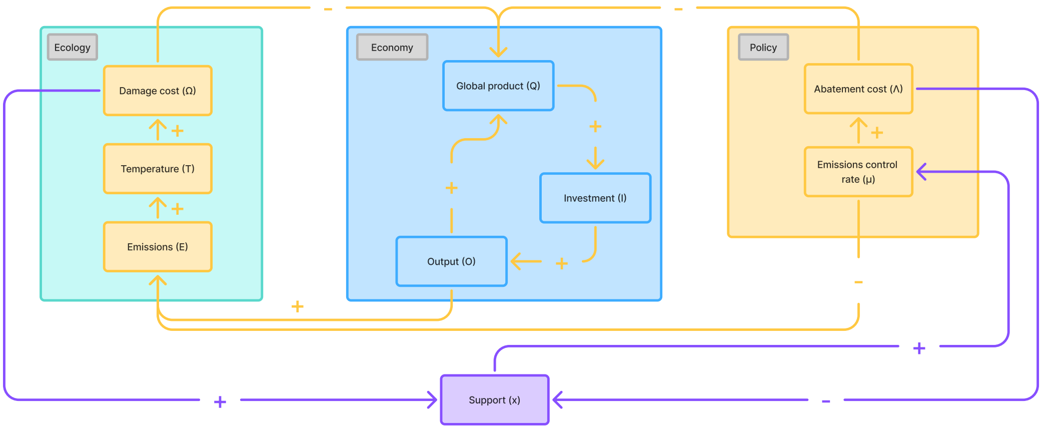

Figure 3.4: Schematic overview of DICE coupled to the social model modelling support dynamics x. '$+$' or '$-$' indicate that an increase in the first variable results in an increase or decrease, respectively, for the second variable.

respectively. Therefore, Λ and Ω are rescaled with coefficients ν_1 and ν_2. These coefficients can be interpreted as a weight on the perception of costs. If $\nu_2 > \nu_1$, the cost of damages are weighted higher than the cost of mitigation. The choice for ν_1 is determined by dividing the maximum value of β (5) by the maximum value of Λ $(\max \theta_1)$, resulting in $\nu_1 = 18.34$. For the choice of ν_2, the value of $f(T)$ and Ω are calibrated at temperature increase 1.5 °C, as this is an important threshold in the literature of climate change, resulting in $\nu_2 = 320.48$. The warming cost function $f(T)$ and damage cost function Ω are both plotted in Figure 3.5. This second coupling results in the following equation for the social dynamics,

$$\frac{dx}{dt} = \kappa x(1-x)(-\nu_1\Lambda + \nu_2\Omega + \delta(2x-1)). \tag{3.39}$$

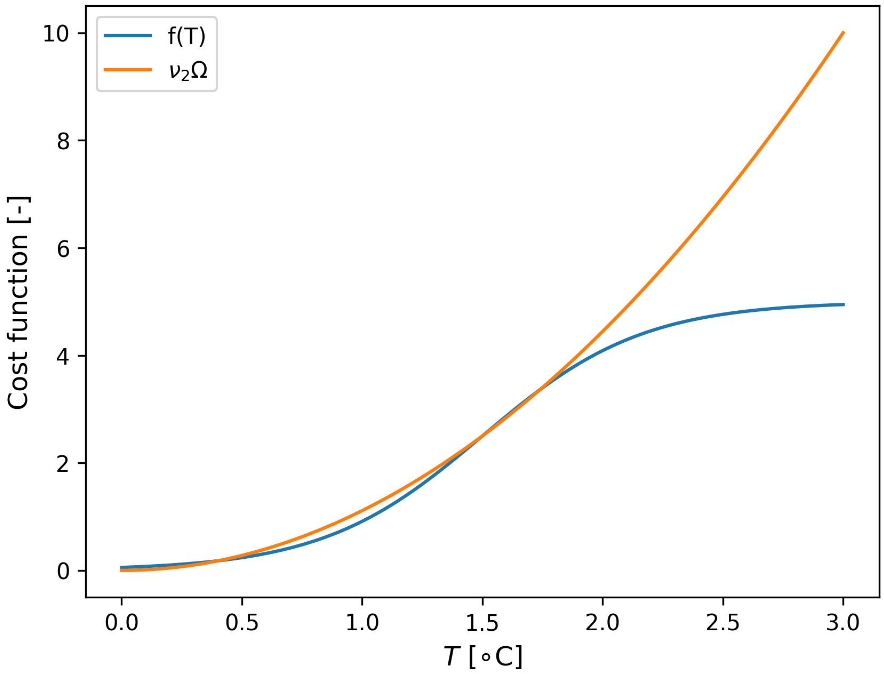

Figure 3.5: Warming cost function $f(T)$ [-] and the rescaled damage cost function Ω [-] with $\nu_2 = 320.48$, plotted against temperature increase T.

Chapter 4

Results of the decoupled models

In chapter 3 we discussed the model DICE-2023 together with adaptations made for this research as well as the social dynamics model. In this chapter we analyse how the models without coupling respond to changes in the various parameters for a better understanding of the models. For this purpose we investigate the development in time and the equilibrium points of these models. The time development of DICE is presented in section 4.1. The analysis of equilibria for DICE for the one timescale can be found in section 4.2. This is continued with the same analysis for the two-timescale method in section 4.3. In section 4.4 the social model is studied with an investigation of the equilibrium points as well as a parameter analysis.

4.1 DICE integrated

DICE is integrated using the equations from section 3.1.1, for more details on the exogenous variables and initial conditions see appendix A. The timestep of DICE-2023 is 5 years and this is used in this thesis as well for verification purposes. A variable of interest from the adapted DICE model, is the atmospheric temperature T_{AT}. For different functions of μ (see Figure 3.3), the time evolution of T_{AT} is plotted in Figure 4.1. μ is a linear function or a hyperbolic tangent, where t_μ - the time needed for μ to become 1 - is varied (more details in section 3.1.3.2). As shown in Figure 4.1, higher values of t_μ lead to higher atmospheric temperatures. This follows from the relation between carbon emissions and atmospheric temperature. For larger t_μ, the cumulative emissions increase, resulting in a higher temperature, as described by the model equations in section 3.1.1.3. This also explains the different results for linear and hyperbolic tangent functions for μ. As shown in Figure 3.3, the

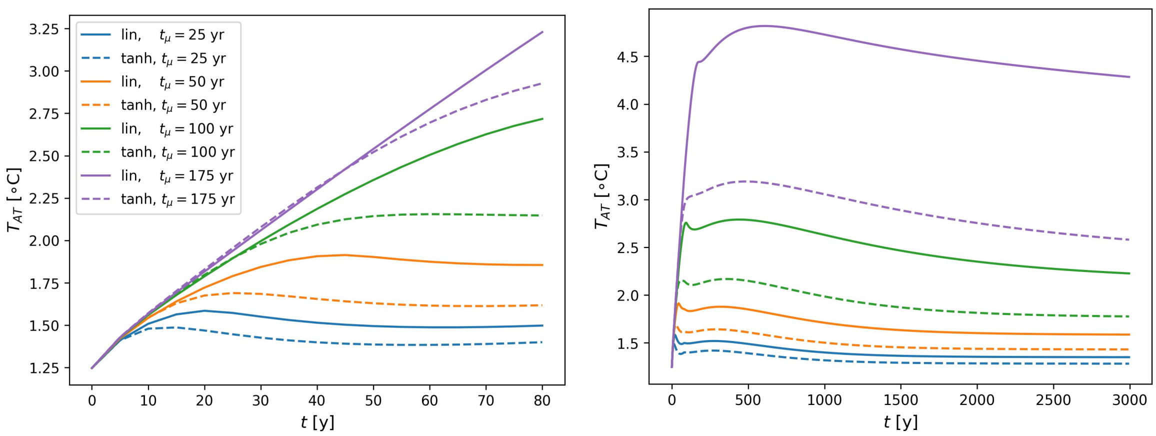

Figure 4.1: The atmospheric temperature T_{AT} of the DICE model for different functions of μ. t_μ is the time needed for μ to become 1.

area under the curve for the hyperbolic tangent is larger, resulting in less carbon emissions. In this figure, the atmospheric temperature seems to stabilize to an equilibrium.

4.2 Equilibrium of DICE with one timescale

We derive the possible equilibria of this model by solving equations 3.27. The first equation of 3.27 shows that a requirement for an equilibrium is that $R_i(t) = 0$. From this we find explicit expressions for the other variables: $M_{AT}(t) = M_{AT}(1765)$, $C_{acc}(t) = C_{tot}$, $T_1(t) = 0.324\ F_{EX}$ and $T_2(t) = 0.44\ F_{EX}$. The results are computed numerically with the Newton-Raphson method for different functions of μ (Figure 4.2). From Figure 4.2 it is clear that the equilibrium atmospheric temperature is not dependent on the evolution of μ, while the accumulated carbon is. This is in line with the analytically derived equilibrium where T_{AT} is a fixed value and C_{acc} depends on the total carbon emissions in history. The derived equilibrium is not, however, the equilibrium we expected to see from the time simulations in Figure 4.1. Due to the requirement that $R_i = 0$ and the decay time of the first reservoir, this equilibrium is reached after approximative million years. Furthermore, it is not a physical feasible equilibrium that all the carbon is stored in the oceans and vegetation and that the atmospheric CO_2 concentration equals pre-industrial levels. One would expect a transport of carbon from the ocean to the atmosphere, but this contradicts the equilibrium. Since the equilibrium is not attained in a time domain of our interest and not physically feasible, the one-timescale method is not applicable. We continue with the 2-timescale method for finding a different equilibrium.

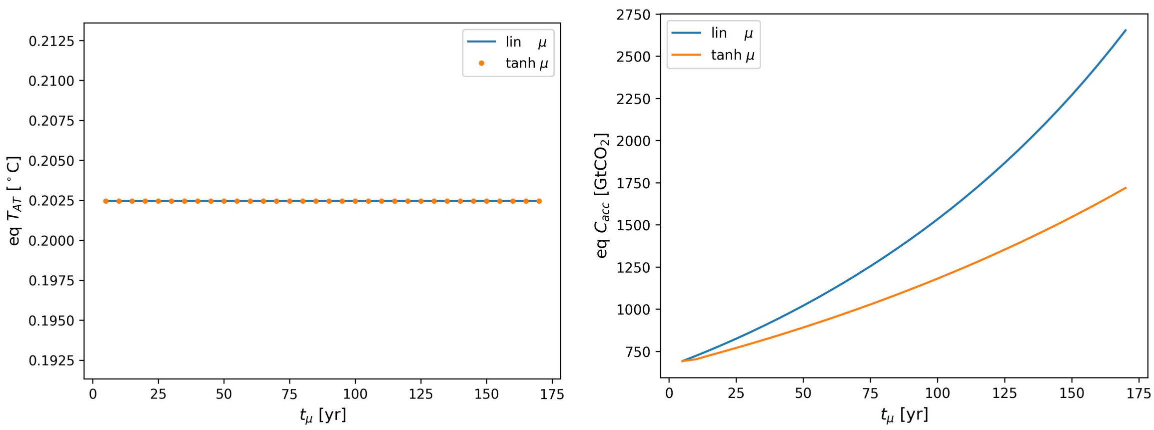

Figure 4.2: The equilibrium value for a) atmospheric temperature T_{AT} and b) accumulated carbon C_{acc} plotted against different values for t_μ; the time needed for μ to go to 1.

4.3 Equilibrium of DICE with the 2-timescale method

We use the 2-timescale method to find a mathematical equilibrium that is close to the apparent stabilization of the temperature visible in Figure 4.1. From Equations 3.35 we can extract the equilibrium solution by setting the derivative with respect to t to zero and setting the slow timescale to the initial time ($\lim\ \tau \to \tau_0$). The equilibrium solution for the 2-timescale method is given in Equations 4.1.

$$\begin{cases}
\lim\limits_{\tau\to\tau_0} R_1^0(\tau) & = R_1^0(\tau_0) \\
\lim\limits_{\tau\to\tau_0} R_2^0(\tau) & = R_2^0(\tau_0) \\
\lim\limits_{\tau\to\tau_0} R_3^0(\tau) & = 0 \\
\lim\limits_{\tau\to\tau_0} R_4^0(\tau) & = 0 \\
\lim\limits_{\tau\to\tau_0} T_1^0(\tau) & = T_1^0(\tau_0) \\
\lim\limits_{\tau\to\tau_0} T_2^0(\tau) & = 0.44F^0(\tau_0) \\
\lim\limits_{\tau\to\tau_0} M_{AT}^0(\tau) & = R_1^0(\tau_0) + R_2^0(\tau_0) + M_{AT}(1765) \\
\lim\limits_{\tau\to\tau_0} C_{acc}^0(\tau) & = C_{tot} - (M_{AT}^0(\tau_0) - M_{AT}(1765)) \\
\lim\limits_{\tau\to\tau_0} F^0(\tau) & = F_{EX} + \eta \log_2\left(\frac{M_{AT}^0(\tau_0)}{M_{AT}(1765)}\right) \\
\lim\limits_{\tau\to\tau_0} T_{AT}^0(\tau) & = T_1^0(\tau_0) + T_2^0(\tau_0) \\
0 & = -(\zeta_0 + \zeta_C C_{acc}^0(\tau) + \zeta_T T_{AT}^0(\tau)) + \sum_{i=1}^3 \alpha^0(\tau)\xi_i\tau_i\left(1 - e^{-\frac{100}{\alpha^0(\tau)\tau_i}}\right) + \alpha^0(\tau)\xi_4\tau_4
\end{cases} \tag{4.1}$$

This equilibrium solution shows that the first two carbon reservoirs R_1 and R_2 are kept constant, whereas the last two carbon reservoirs R_3 and R_4 are set to zero. The temperature T_1 is constant and the temperature T_2 depends on the total carbon emissions throughout the years. The choice for the initial time τ_0 (and with that the initial condition) plays an important role for the equilibrium solution; since three variables are constant and therefore equal to the initial condition. The role of τ_0 is shown in the schematic overview of how the 2-timescale method is applied to DICE (Figure 4.3). First, the adapted DICE model is integrated in time while there are still carbon emissions E. At a certain time t_μ the carbon emissions stop. Note that we are interested in finding equilibria for $t \geq t_\mu$, as discussed in 3.1.4.1. In this time domain at some τ_0 the model DICE is replaced with the 2-timescale system of equations. This is done by using the values of DICE at τ_0 as initial conditions for the 2-timescale system. From the 2-timescale system of equations an equilibrium is derived via Equations 4.1.

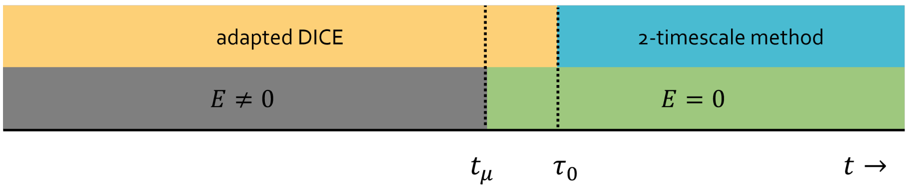

Figure 4.3: Schematic overview of the implementation of the 2-timescale method

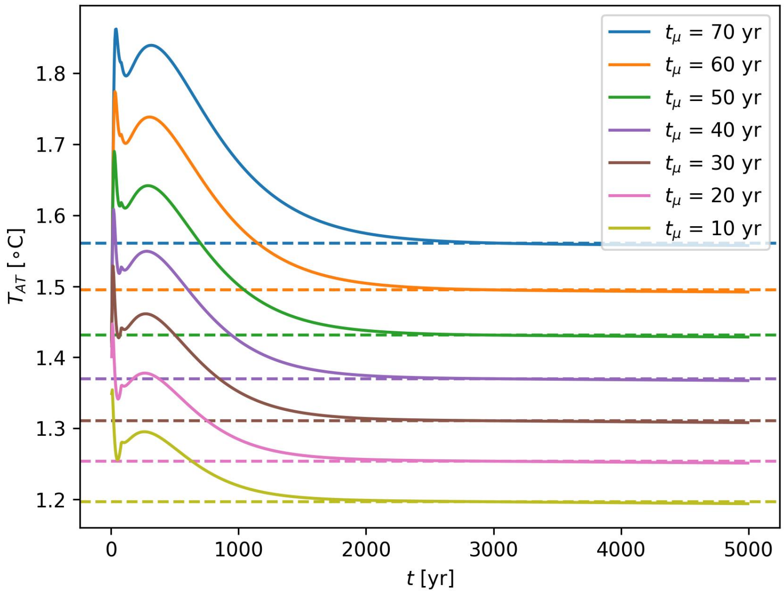

Figure 4.4: Time evolution of atmospheric temperature T_{AT} with DICE (solid lines) for different values of t_μ with μ the hyperbolic tangent. The equilibrium for atmospheric temperature found with the 2-timescale method with τ_0 are represented with dashed lines.

After the carbon emissions equal zero at t_μ, the atmospheric temperature is still fluctuating due to processes on a slower timescale. For this reason τ_0 is chosen to be 3000 years. We show how the equilibrium found with this τ_0 compares to the visual equilibriums of DICE. In Figure 4.4 the time evolution of the adapted DICE model for the atmospheric temperature is shown with μ a hyperbolic tangent with different values of t_μ. The equilibrium found with the 2-timescale method is plotted with dashed lines using the corresponding values of t_μ. The results for the linear μ function are similar to the results for the hyperbolic tangent μ - but the temperatures are slightly shifted due to more carbon emissions - and therefore omitted for this report. From the figure it is visible that the dashed lines are close to the visual equilibrium. For larger values t, the equilibrium found with the 2-timescale method has a small offset with respect to the time evolution of the adapted DICE.

4.4 Social dynamics

The social model that describes the dynamics of the fraction of mitigators x is discussed in section 3.2. The model equation is adapted to Equation 3.39 to support the coupling. The latter is repeated below,

$$\frac{dx}{dt} = \kappa x(1-x)(-\nu_1\Lambda + \nu_2\Omega + \delta(2x-1)).$$

κ is the social learning rate, δ the strength of the social norms, Λ the mitigation cost and Ω the damage cost as fraction of the global economy. Parameters ν_1 and ν_2 are the perceived weights for these costs. In section 4.4.1 the equilibria and their stability are studied to better understand the social dynamics model. In section 4.4.2 we discuss the sensitivity of the model parameters on the social dynamics.

4.4.1 Equilibria and stability

In this section the equilibria and stability for the social model are determined for a better understanding. In order to simplify the analysis, we introduce,

$$\psi := -\nu_1\Lambda + \nu_2\Omega. \tag{4.2}$$

This results in the following equation,

$$f(x,\psi) = \kappa x(1-x)(\psi + \delta(2x-1)). \tag{4.3}$$

From Equation 4.3 it follows that there are three equilibria: $x_1 = 0$, $x_2 = 1$ and $x_3 = \frac{1}{2}\left(1 - \frac{\psi}{\delta}\right)$. To investigate the stability of these equilibria we determine the derivative with respect to x.

$$f_x(x,\psi) = \kappa(\psi - \delta) + 2\kappa x(3\delta - \psi) - 6\kappa\delta x^2 \tag{4.4}$$

From Equation 4.4, we find that x_1 is stable for $\psi < \delta$ and unstable for $\psi > \delta$. The second equilibrium x_2 is unstable for $\psi < -\delta$ and stable for $\psi > -\delta$. For positive δ, the third equilibrium is unstable for $|\psi| < \delta$ and stable otherwise. Maghsoodlo et al. [10] found the same results for the first two equilibrium points and their stability, as well as a third unstable equilibrium in the range [0,1]. The derived equilibria and their stability are presented in Figure 4.5.

We show that there are transcritical bifurcations at $(\psi_0, x_0) = (-\delta, 1)$ and $(\delta, 0)$. There are five requirements for a transcritical bifurcation [37]:

1. $f(x,\psi) = 0$,

2. $\frac{\partial f}{\partial x}(x, \psi) = 0$,
3. $\frac{\partial f}{\partial \psi}(x, \psi) = 0$,
4. $\frac{\partial^2 f}{\partial x \partial \psi}(x, \psi) \neq 0$,
5. $\frac{\partial^2 f}{\partial x^2}(x, \psi) \neq 0$.

The first two requirements are already shown in the analysis above. We determine the value of $f_\psi(x, \psi)$ for the two points in question,

$$f_\psi(x, \psi) = \kappa x(1 - x). \tag{4.5}$$

Indeed, $f_\psi(0, \delta) = f_\psi(1, -\delta) = 0$. The second derivatives of the last two requirements are:

$$\frac{\partial^2}{\partial x \partial \psi}(x, \psi) = \kappa(1 - 2x), \tag{4.6}$$

$$\frac{\partial^2 f}{\partial x^2}(x, \psi) = 2\kappa(3\delta - \psi) - 12\kappa\delta x. \tag{4.7}$$

The points $(\psi_0, x_0) = (-\delta, 1)$ and $(\delta, 0)$ are both non-zero for these second derivatives, provided that κ and δ are non-zero. We conclude that the two points are transcritical bifurcations.

In the case that $\delta = 0$, the third equilibrium becomes a vertical line with $\psi = 0$ for every x. When this happens, only the value of ψ determines which equilibrium is stable. There is no longer a range for values of ψ where two equilibria are stable and the value of x puts the model in one of the two regions of attraction.

From the analysis of the equilibrium solutions, it is clear that the relation between ψ and δ is an important factor in the social dynamics model. In Figure 4.6 the value of x after 80 years is plotted for multiple combinations of ψ and δ. This is done with x at a starting point $x_0 = 0.05$ and $x_0 = 0.95$. In the case $x_0 = 0.05$ (Figure 4.6a), we see that a front distinguishes between the model converging to 0 or 1. This corresponds with the stability analysis that for $\psi > \delta$ the solution $x = 0$ becomes unstable. We expect to see this behaviour in the figure for $x_0 = 0.05$, as this is close to the equilibrium of $x = 0$. The front in Figure 4.6b is changed in orientation. In a similar way, this confirms the result from the stability analysis that $\psi < -\delta$ leads to the solution $x = 1$ becoming unstable. The gradient for x between 0 and 1 shows that the model has not yet converged to an equilibrium; experiments with a longer runtime present a sharper front.

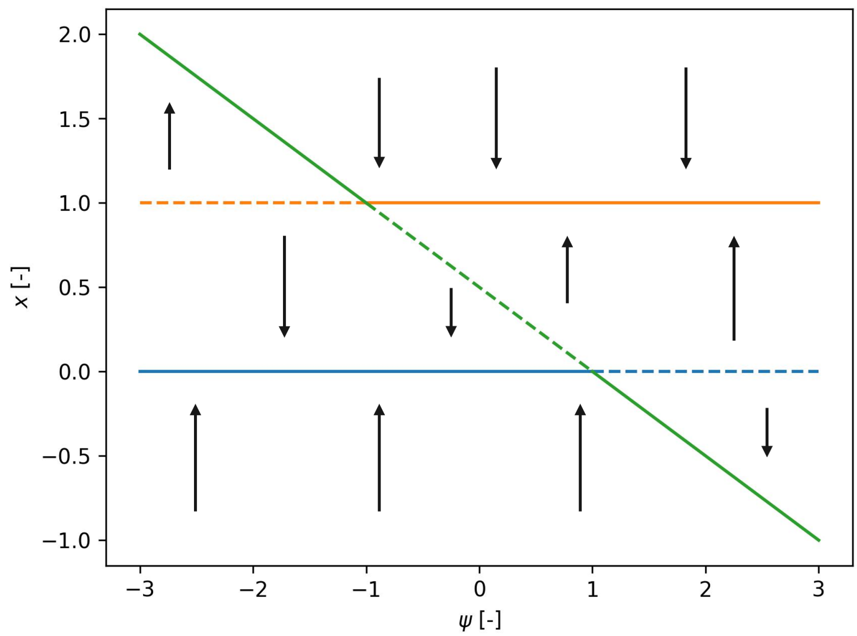

Figure 4.5: Algebraically derived bifurcation diagram of the fraction of mitigators x for the parameter $\psi := -\beta + f(T)$ with $\delta = 1$. ψ is a representation of the cost for mitigation. The solid and dashed lines represent stable and unstable equilibria respectively. At $(\psi, x) = (-\delta, 1)$ and $(\delta, 0)$ there are transcritical bifurcations.

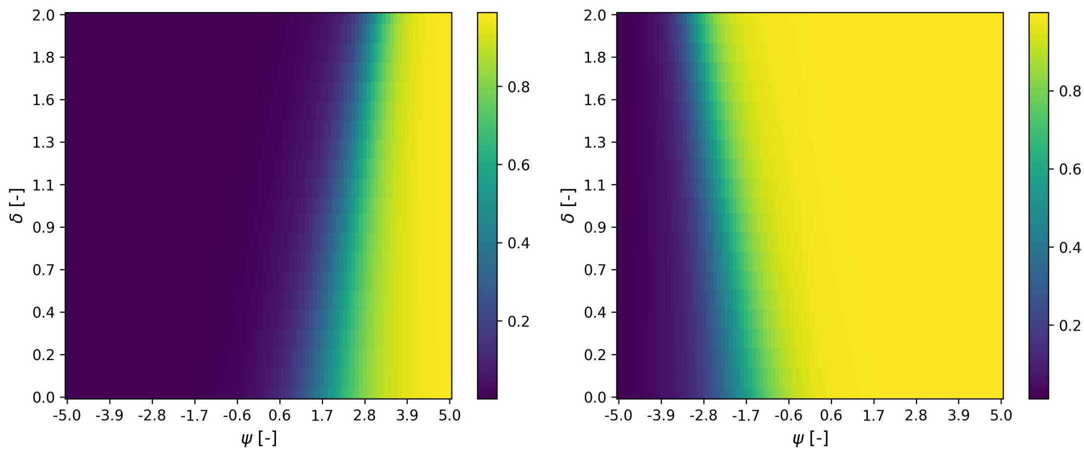

(a) $x_0 = 0.05$ (b) $x_0 = 0.95$

Figure 4.6: The value of x after a simulation of 80 years for different combinations of ψ and δ and 0.05 and 0.95 as initial conditions for x.

4.4.2 Parameter analysis

A parameter analysis was performed to have a better understanding of the model. The differential Equation 3.36 is integrated with backward Euler (with the forward Euler as initial guess). For the integration $\Delta t = 5$ years is used to synchronise this with DICE. For some runs of this model these steps were too large to find a solution, here linear interpolation was used. The results are shown in Figure 4.7. Unsurprisingly, the value of x remains constant when $\kappa = 0$ in Figure 4.7a. Larger values

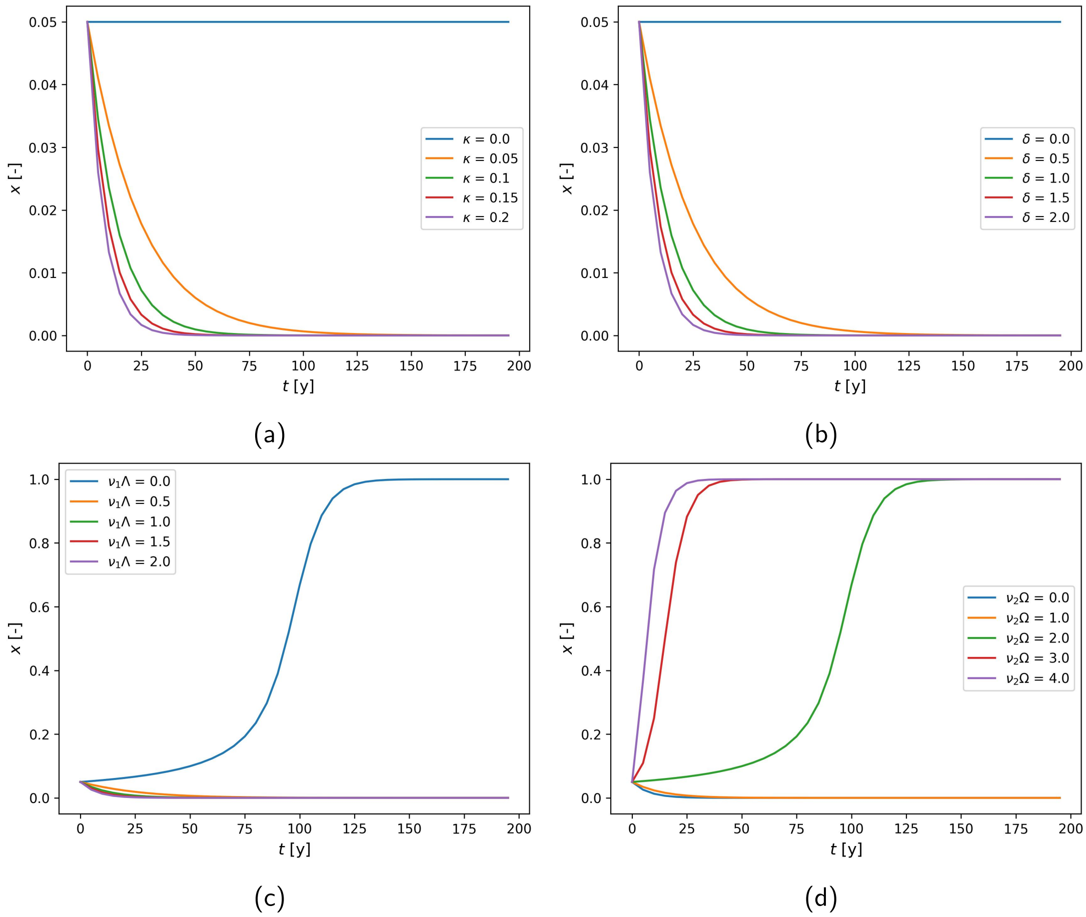

Figure 4.7: The time progression of the fraction of mitigators x from the behaviour model [10] for different values for the model parameters and variables. In a) social learning rate κ [y^{-1}], in b) strength of social norm δ, in c) perceived mitigation cost $\nu_1\Lambda$ and in d) perceived damage cost $\nu_2\Omega$ are varied. The default parameters for this experiment are: $\kappa = 0.1$ per year, $\delta = 1$, $\nu_1\Lambda = 1$ and $\nu_2\Omega = 1$.

of κ increase the speed of convergence towards $x = 0$. The stronger the social norms δ, the faster the convergence of the support level to the largest group (non-mitigators), as visible in Figure 4.7b. In Figure 4.7c a larger value of $\nu_1\Lambda$ - the perception of mitigation costs - pushes the support faster to $x = 0$. In the case without mitigation costs ($\nu_1\Lambda$), the support converges to another solution $x = 1$. Here we see tipping happening as described in section 4.4.1; the absence of mitigation costs causes

ψ to become larger than δ. More tipping behaviour is shown in Figure 4.7d for values $\nu_2\Omega \geq 2$. This is caused by the same reason of ψ being larger than δ. What is interesting to note is that the higher the value of $\nu_2\Omega$, the faster the convergence. This follows directly from the model equation 3.39.

Chapter 5

Results of the coupled model

This chapter discusses the results of the coupling between the adapted DICE-2023 and the social model for support levels, described in section 3.3. In particular, multiple parameters are varied and the corresponding results discussed. The parameters are the following: social learning rate κ, strength of social norms δ, perception of mitigation and damage costs ν_1, ν_2 and bounds on the rate of change for emission control rate μ; $\Delta\mu_{min}$ and $\Delta\mu_{max}$. If not specified, default values for the parameters are used in the experiments. These values are shown in Table 5.1. In DICE-2023 the emission control rate μ has an initial condition of 0.05, the initial condition for public support for climate policy is chosen to be the same value. The model parameters of the social model δ and κ are set to the maximum value of the range suggested by Maghsoodlo et al. [10]. The choices for the value of ν_1 and ν_2 are described in section 3.3. The minimum bound for change in emission control rate μ is set to 0.0 yr^{-1}, to take into account the limited supply of fossil fuels. The maximum bound is set to 0.04 yr^{-1} to consider the technical feasibility of rapid change in emissions. By varying these parameters, we investigate if these choices for the parameters of the coupling significantly influence the model results.

Table 5.1: Default parameter values for the experiments

Parameter	Symbol	Value	Unit
Initial condition public support for climate policy	x_0	0.05	-
Social learning rate	κ	0.2	yr^{-1}
Strength of social norms	δ	2	-
Perceived weight mitigation cost	ν_1	18.34	-
Perceived weight damage cost	ν_2	320.48	-
Minimum change in emission control rate	$\Delta_{\mu_{min}}$	0.0	yr^{-1}
Maximum change in emission control rate	$\Delta_{\mu_{max}}$	0.04	yr^{-1}

5.1 Sensitivity analysis

The first parameter we vary is social learning rate κ. Important variables to analyse in the coupled model are: the atmospheric temperature T_{AT}, support level for climate policy x, emission control rate μ and perceived balance between mitigation cost and damage cost ψ (Equation 4.2). These variables are plotted against time for varying values of social learning rate κ in Figure 5.1. The social learning rate κ accelerates or delays the support dynamics as visible in the plot of x (Fig. 5.1d); $x = 1$ is reached earlier for $\kappa = 0.2$ yr^{-1}. The plot for ψ (Fig. 5.1b) shows that all values of ψ are larger than δ $(= 2)$, this causes the support levels x to rise. The value of x determines how much the emission control rate μ (Fig. 5.1c) rises; a high value of x means a large change in μ, a small value of x a small change. In the case of $\kappa = 0$, the support remains at $x = 0.05$ and zero emission is reached (t_μ) after approximately 500 years. The atmospheric temperature increase in the year 2100 (80 years from the start of the model) and the 2-timescale equilibrium are shown in Figure 5.2. In Figure 5.2 it is visible that from around $\kappa = 0.025$ yr^{-1} the equilibrium of the 2-timescale method remains below 2 °C and from around $\kappa = 0.075$ yr^{-1} the same holds for the 2100 atmospheric temperature increase. The t_μ for these processes are 65 and 45 years, respectively. For most values of κ, the temperature at 2100 is higher than the temperature at equilibrium. This is, however, not the case for small values of κ; the 2100 temperature remains below 4 °C and the equilibrium temperature approaches a 14 °C difference. The high temperature of the equilibrium should not be considered as an accurate description of global warming. But rather as an indication that the peak of the temperature is not yet reached at year 2100 and that the temperature might rise after 2100.

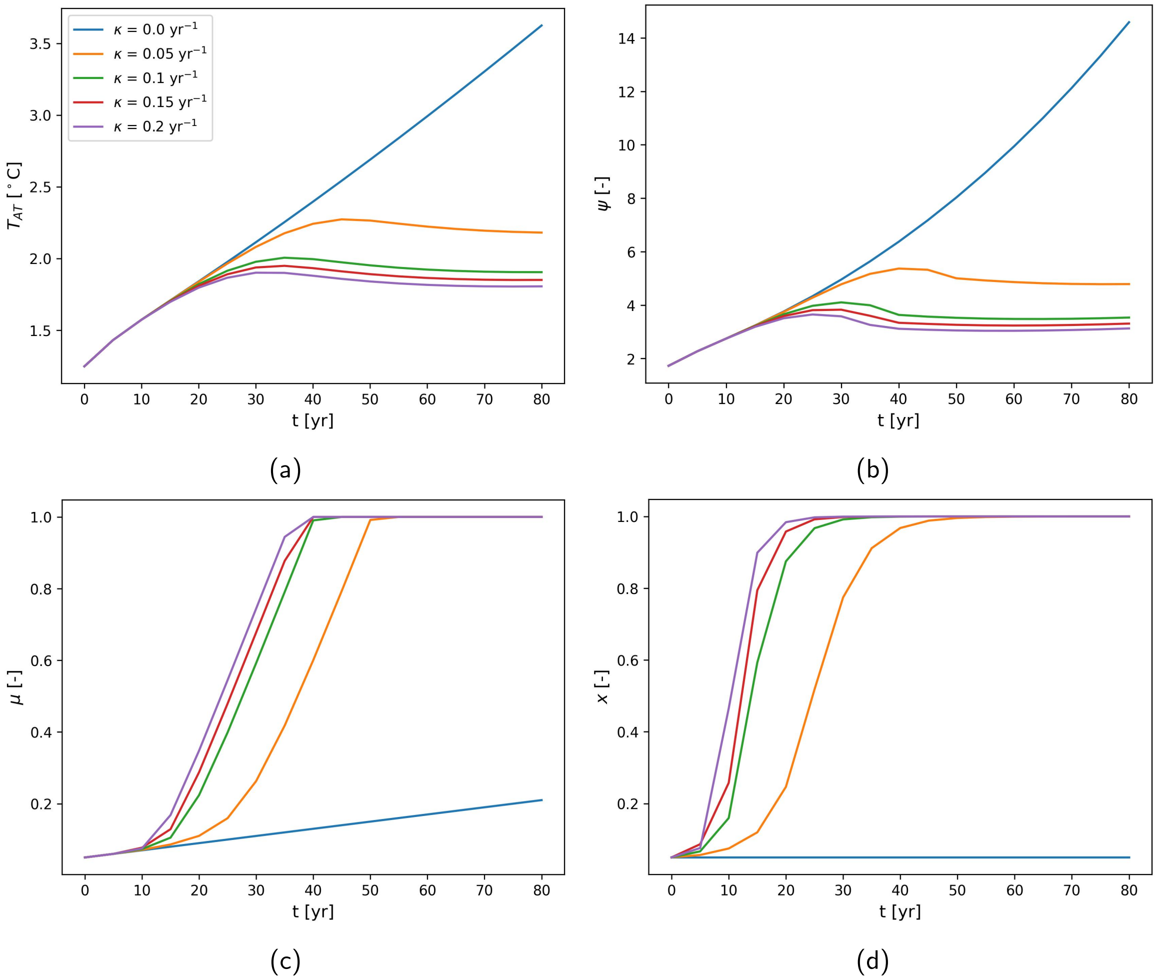

Figure 5.1: Atmospheric temperature T_{AT}, perceived balance between mitigation cost and damage cost ψ, emission control rate μ and support level for climate policy x plotted against time for varying values of social learning rate κ.

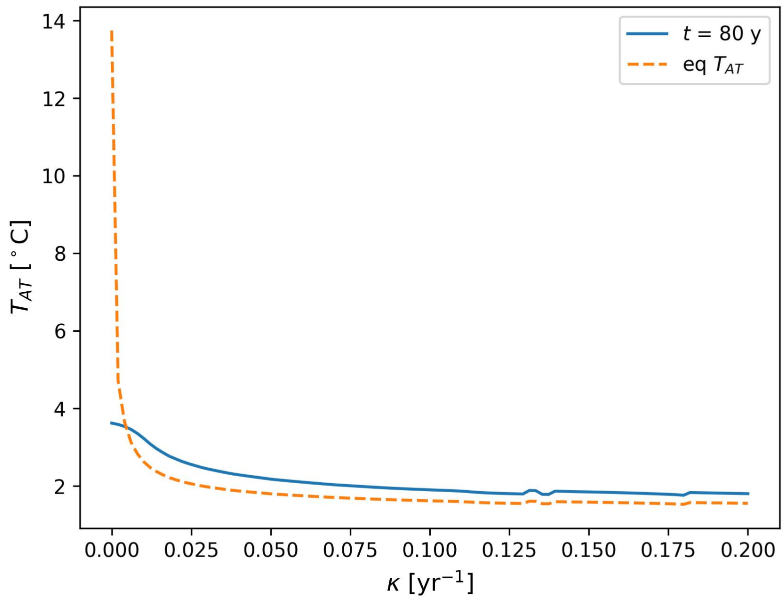

Figure 5.2: The value of atmospheric temperature T_{AT} at year 2100 (80 years from the start of the model run) and the equilibrium temperature for the 2-timescale method plotted against social learning rate κ.

In section 4.4.1 it is shown that the value of ψ $(:= -\nu_1\Lambda + \nu_2\Omega)$ relative to δ is determinant for the equilibrium that will be reached for x. For this reason we now investigate the influence of δ, ν_1 and ν_2 on the atmospheric temperature. Figure 5.3 shows the relation between δ and T_{AT} for varying values of x_0. If the initial support level x_0 is low, high strength of social norms delay climate action and the equilibrium atmospheric temperature rises substantially (Fig. 5.3a). The 2100 temperature remains at 4 °C. This value is probably the maximum temperature increase that DICE produces for the year 2100, and hence represents the worst-case scenario. For support levels $x_0 \geq 0.5$, the strength of social norms has only a small influence on the atmospheric temperature (Fig. 5.3c). In the case where initial support is close to 0.5, both these relations are visible (Fig. 5.3b). In this case for δ approximately smaller than 30, the temperature remains in the range of 2 °C difference and for larger δ, we see a similar behaviour as in Figure 5.3 a).

Figure 5.4 shows the influence of ν_1 and ν_2 on the atmospheric temperature T_{AT}. It appears that the atmospheric temperature only depends on the value of ν_2. Especially for small values of ν_2 the temperature difference is high.

In order to better understand this behaviour, ψ is plotted over time for varying values of ν_1 and ν_2 in Figure 5.5. Regardless of the value of ν_1 (fig 5.5a), one can see that the initial value of ψ

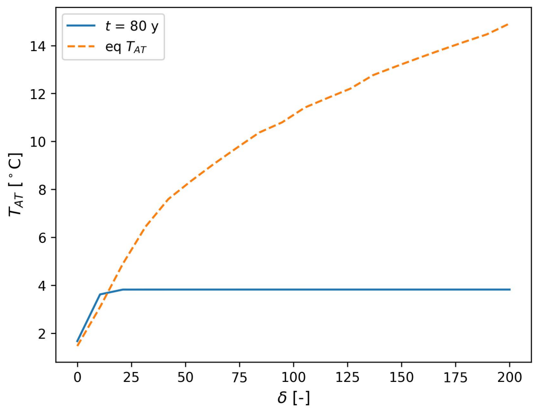

(a) $x_0 = 0.05$

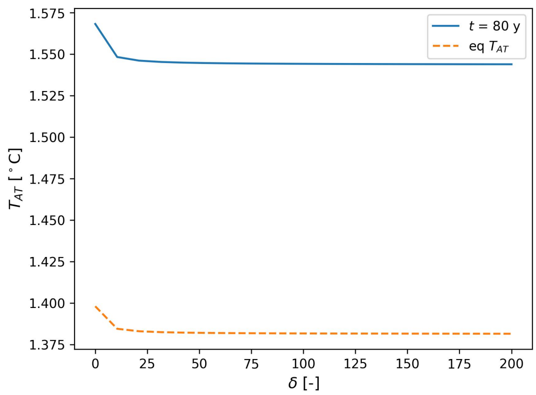

(b) $x_0 = 0.5$

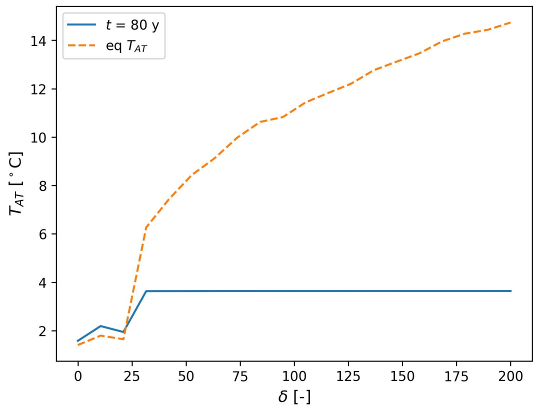

(c) $x_0 = 0.45$

Figure 5.3: The value of atmospheric temperature T_{AT} at year 2100 (80 years from the start of the model run) and the equilibrium temperature for the 2-timescale method plotted against the strength of social norms δ for different starting values for support x_0.

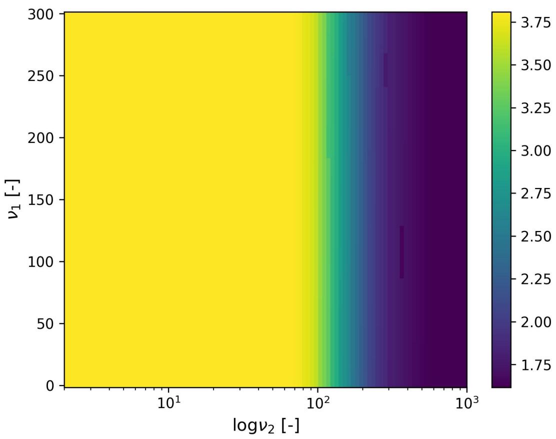

(a)

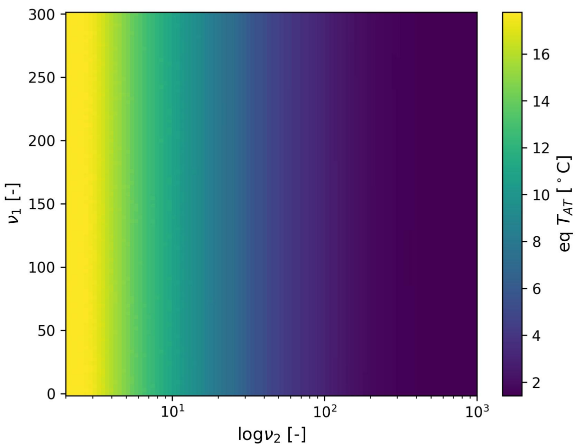

(b)

Figure 5.4: a) The value of atmospheric temperature T_{AT} at year 2100 (80 years from the start of the model run) and b) the equilibrium value with the 2-timescale method for the atmospheric temperature T_{AT} [°C] plotted for multiple values of ν_1 and ν_2.

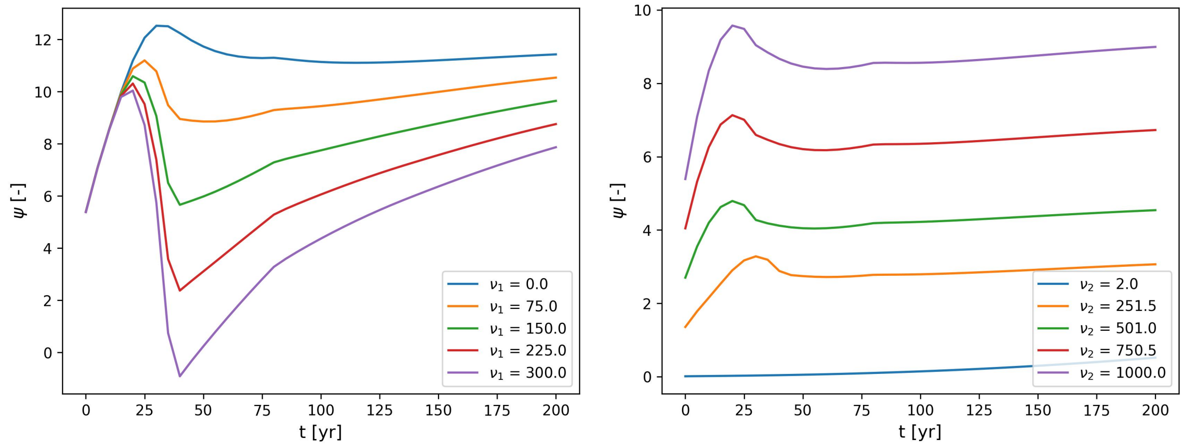

(a) (b)

Figure 5.5: The value of ψ plotted against time for varying values of ν_1 and ν_2.

is high. Since in this case $\psi > \delta$, the solution $x = 0$ becomes unstable and the public support increases towards the stable solution $x = 1$. Due to the increasing support, the emissions control rate μ increases as well. This leads to increasing mitigation costs (represented by the dip in ψ in the graph). At this moment in time, the support is close to 1 and the high mitigation costs are not enough incentive to change the public support, i.e. ψ remains above $-\delta$. Higher values of ν_1 could cause the solution $x = 1$ to become unstable and decrease public support. However, even with decreasing public support, the default parameters of this model run prevent a decrease in climate policy ($\Delta_{\mu_{min}} = 0.0$ yr^{-1}, Table 5.1). For varying ν_2 (fig 5.5b), most values of ψ are high which leads to a similar process as described before. However for $\nu_2 = 2$, the initial value of ψ is small as the damage costs have a small weight in the decision making. After around 400 years, ψ crosses the value of δ and support increases. This delay in support translates to delay in climate policy, which explains the high temperature difference in Figure 5.4.

In the coupling between public support x and emissions control rate μ - a parameter representing climate policy and technical ability - values for $\Delta\mu_{min}$ and $\Delta\mu_{max}$ were chosen. Figure 5.6 shows the relation between these bounds $\Delta\mu_{min}$ and $\Delta\mu_{max}$ and atmospheric temperature increase. Figure 5.6a) shows that the difference in temperature is relatively low for varying values of $\Delta\mu_{min}$. The reason could be that the support changes quickly to $x = 1$, resulting in a short time where μ is changed at the minimal rate. As can be seen in Figure 5.6 b), the temperature difference is high for small values of $\Delta\mu_{max}$. This is a representation of the situation where support for climate action is high, but the industry is restricted with regard to increasing μ (for example due to technical difficulties or shortages in materials). From about a $\Delta\mu_{max}$ of 0.02 yr^{-1} the temperature difference

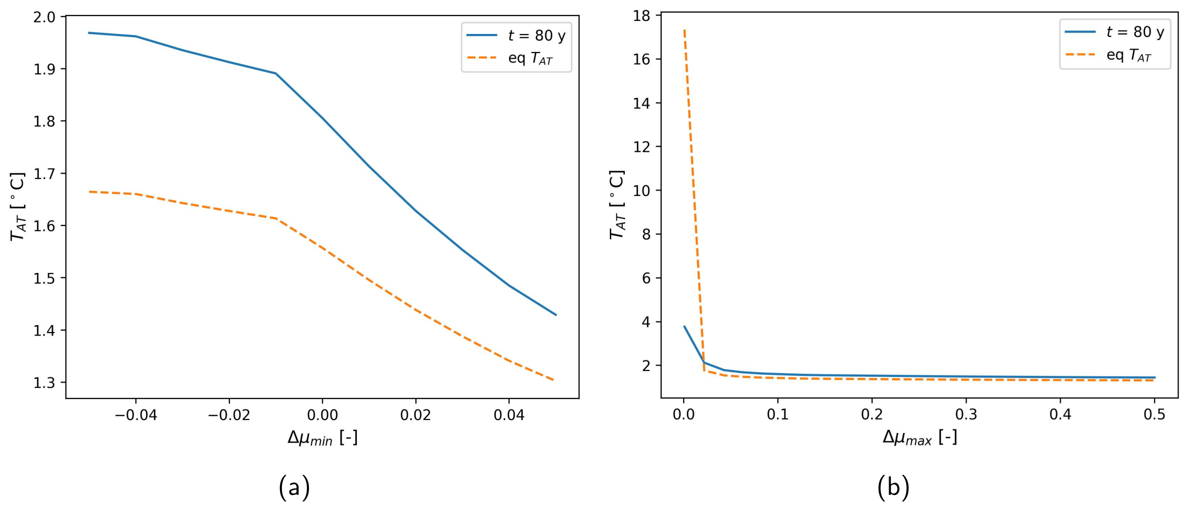

Figure 5.6: The value of atmospheric temperature T_{AT} at year 2100 (80 years from the start of the model run) and the equilibrium value with the 2-timescale method for the atmospheric temperature T_{AT} plotted against a) $\Delta\mu_{min}$ and b) $\Delta\mu_{max}$.

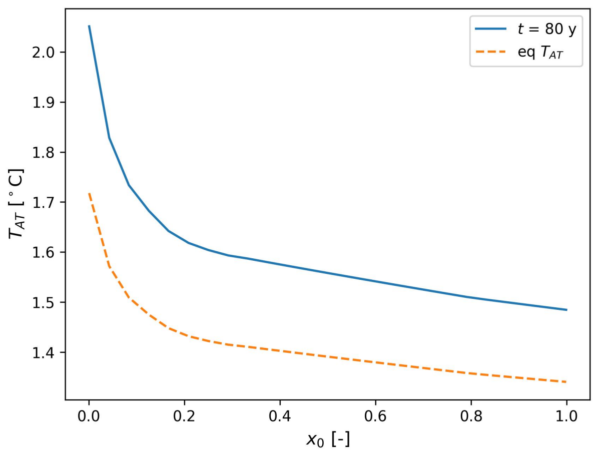

Figure 5.7: The value of atmospheric temperature T_{AT} at year 2100 (80 years from the start of the model run) and the equilibrium value with the 2-timescale method for the atmospheric temperature T_{AT} plotted against initial support x_0.

remains around 2 °C.

The last value that is investigated is that of initial public support x_0. The results of varying x_0 are shown in Figure 5.7. It can be seen that the temperature decreases with increasing x_0. This could be because for higher x_0, μ converges faster to 1 which leads to less carbon emissions overall. However, the relative difference for the atmospheric temperature is small. This is probably influenced by the choice for the default parameters in Table 5.1. Different parameter values can shift the sensitivity of the initial condition.

5.2 Tipping in the coupled model

5.2.1 Investigating tipping behaviour

In section 4.4.1 we found transcritical bifurcations in the social model. Some results (the sensitivity analysis of ν_2 (Fig. 5.4) and δ (Fig. 5.3)) in this chapter could indicate a bifurcation in the coupled model as well. To further investigate this hypothesis, some additional simulations are performed with varying values of ν_2 and x_0, the results are shown in Figure 5.8. The solid lines start at $x_0 = 0.1$ and the dashed lines start at $x_0 = 0.3$. The bifurcation diagram from Figure 4.5 is shown in the top panels (Fig. 5.8a and b) with black lines. In the top left panel (Fig. 5.8a), the 80 year simulation is shown with x plotted against ψ. For the value $\nu_2 = 2$, the blue lines converge to $x = 0$. This happens because the low value of ν_2 results in a low value of ψ, which puts the simulation in the domain of attraction for the equilibrium solution $x = 0$ (as long as $\psi < \delta$). Initially, this is also the case for the orange lines (ν_2=100). Eventually, the unstable equilibrium solution is crossed and the simulation tips to the equilibrium solution $x = 1$. For the value $\nu_2 = 200$, the green dashed line starts in the domain of attraction of equilibrium solution $x = 1$, but the green solid line starts in the domain of attraction for equilibrium $x = 0$. Higher values of ν_2 (purple lines), result in the simulation starting in the domain of attraction for $x = 1$ and converging quickly to this equilibrium. In the middle and bottom left panel (Fig. 5.8c and e), it is shown that for simulations initially converging to $x = 0$, the temperature after 80 years is significantly higher. The delay in implementation of climate policy is a cause for higher atmospheric temperatures.

In the bottom left panel of Figure 5.8 the relation between atmospheric temperature at 2100 and ν_2 is shown. This is done for two values for x_0; $x_0 = 0.1$ the solid line and $x_0 = 0.3$ the dashed line. At $\nu_2 = 320$, the difference between these two lines is not large. This is in correspondence with the relations displayed in Figure 5.7. For values of ν_2 around 150, there is a more significant difference in the solid and dashed line. This shows that the influence of x_0 is more important for these parameter settings.

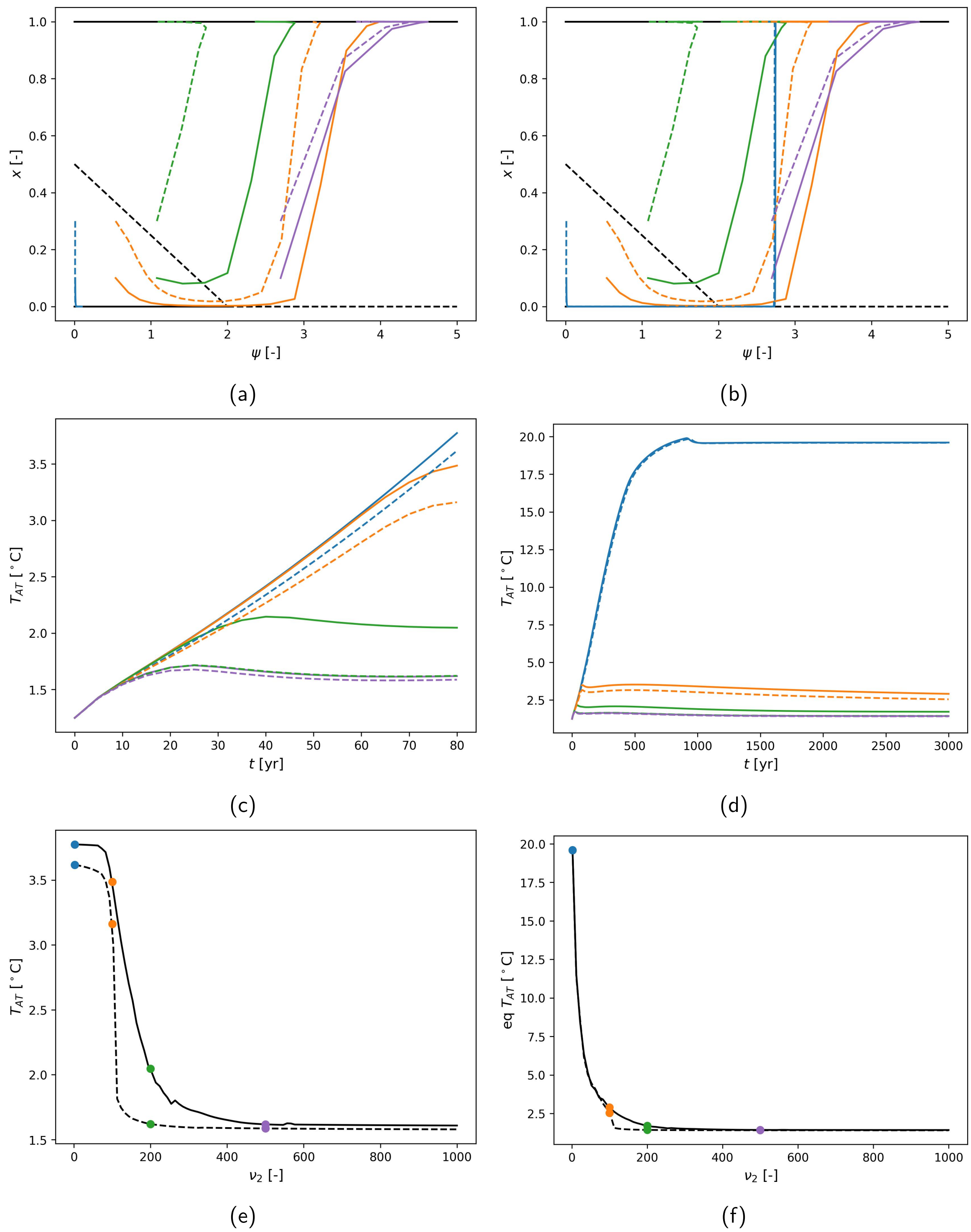

Figure 5.8: Simulations plotted for different values of perception of damage cost ν_2. The simulations are performed with two initial conditions for x_0; $x_0 = 0.1$ (solid lines) and $x_0 = 0.3$ (dashed lines). In the top panels (a and b), the fraction of supporters for climate policy x are plotted against ψ, the balance between perceived costs of mitigation cost and damage cost. The black lines in the top figure represent the bifurcation diagram of the social model. In the middle panels (c and d), the atmospheric temperature T_{AT} is plotted against time. The left panels (a, c and e) are for time simulations for 80 years and the right panels (b, d and f) are time simulations for 3000 years. In the bottom left panel (e), the temperature after 80 years and in the bottom right panel (f), the equilibrium found with the 2-timescale method for t_μ=3000 years is plotted against ν_2.

The right panels (Fig. 5.8b, d and f) show the simulations for 3000 years. The blue lines in the top right panel (Fig. 5.8b) differ from the top left panel (Fig. 5.8a); after converging to $x = 0$ there is tipping at $\psi = 2$, reached around 450 years. The stability of the solution changes from stable to unstable around this point. For the bottom right panel (Fig. 5.8f), the 2-timescale method is applied after the 3000 year simulation to find the equilibrium for the atmospheric temperature. In both the middle and bottom right panels (Fig. 5.8d and f), the (blue) simulation with $\nu_2 = 2$ results in a high atmospheric temperature, consistent with Figure 5.4.

In Figure 5.3 we saw that the relation between atmospheric temperature and δ changed for different values of x_0. This is further illustrated in Figure 5.9, where the simulations for x plotted against ψ for various values of ν_2 and x_0 (similar Figure 5.8a) are repeated for different values of δ. The unstable equilibrium between $x = 0$ or $x = 1$ (dashed black line) changes with the value of δ. This causes the tipping to change as well; in Figure 5.9a high values of ν_2 do not show tipping behaviour and in Figure 5.9d they do. In the range $(-\delta, \delta)$ for ψ, the value of x_0 determines in which region of attraction the simulation starts and plays an important role in the resulting temperature. Outside this range the influence of x_0 is small.

Dependent on the value of δ, the model simulations for different values of ν_2 and x_0 show tipping or no tipping in support level x. We show the atmospheric temperature for these simulations in Figure 5.10. For $\delta = 4$, Figure 5.9c shows an initial drop for values $\nu_2 = 2$ till 200. In Figure 5.10 the temperature is relatively high for these values with respect to the simulation with $\nu_2 = 500$ that did not experience an initial drop. As such, Figure 5.10 confirms earlier results (Figure 5.8a and b) that an initial drop in public support directly results in a high atmospheric temperature. Furthermore, in most cases the simulations starting at $x_0 = 0.1$ result in higher temperatures than simulations starting at $x = 0.3$.

5.2.2 Different types of tipping

In the previous section we saw multiple model simulations with tipping behaviour. In this section we identify the type of tipping for these model simulations. In particular, we focus on the tipping of model simulations in Figure 5.8b and Figure 5.9b.

We see bifurcation-induced tipping when the model run first converges to the equilibrium of $x = 0$ and switches to $x = 1$ at the bifurcation point $(\psi, x) = (\delta, 0)$. This is shown by the orange solid line ($\nu_2 = 100$) in both figures and the blue lines ($\nu_2 = 2$) for the 2-timescale equilibrium in Figure 5.8b.

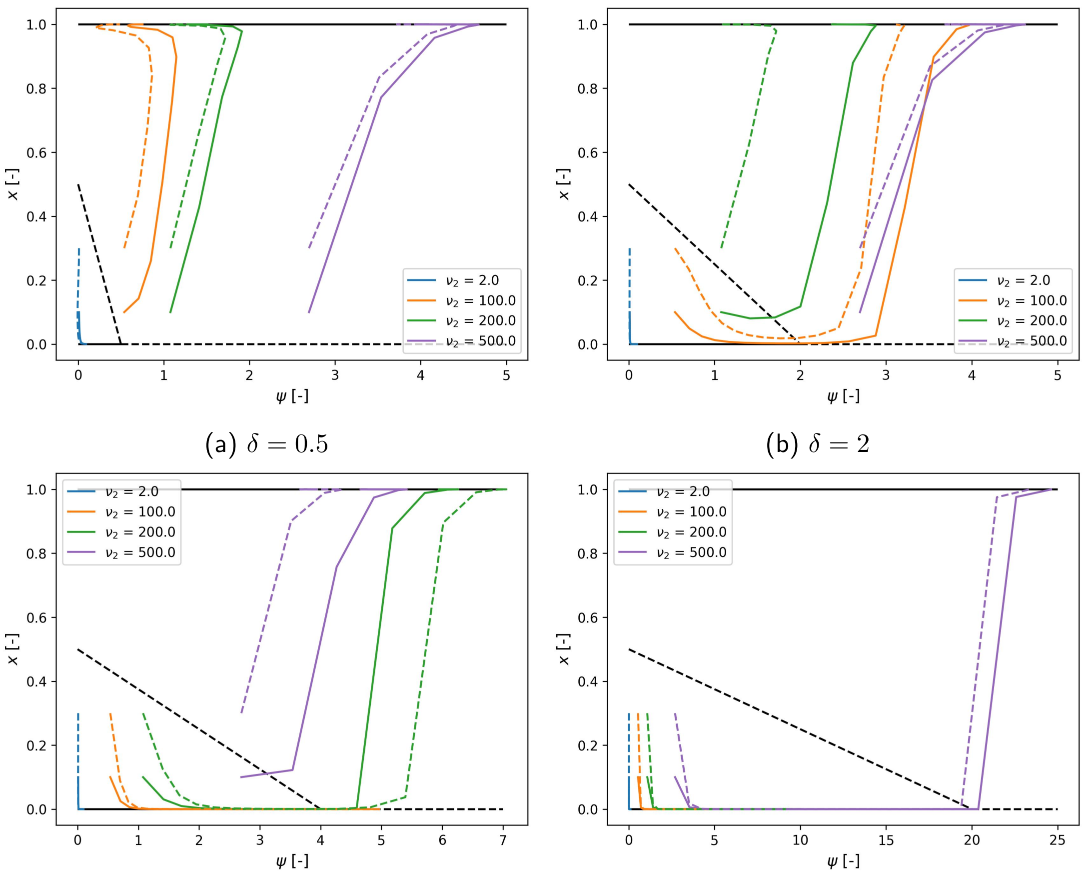

(a) $\delta = 0.5$

(b) $\delta = 2$

(c) $\delta = 4$

(d) $\delta = 20$

Figure 5.9: Public support for climate policy x plotted against ψ, the balance between perceived costs of mitigation cost and damage cost. This is plotted for multiple simulations for varying ν_2. The simulations shown with solid lines start at $x_0 = 0.1$ and the dashed lines at $x_0 = 0.3$. In the subfigures the value of δ is changed.

Rate-induced tipping for this model is controlled by the rate of change in ψ. For fast changes in ψ, the simulation crosses the unstable equilibrium and converges to $x = 1$. The green solid line shows an example of this behaviour. For slow changes in ψ, the simulation does not cross the unstable equilibrium and converges to $x = 0$. This is shown for the blue dashed line. The rate of change in ψ is not externally controlled in this model. But even though it is endogenously determined, it still plays an important role in the crossing or not of the unstable equilibrium.

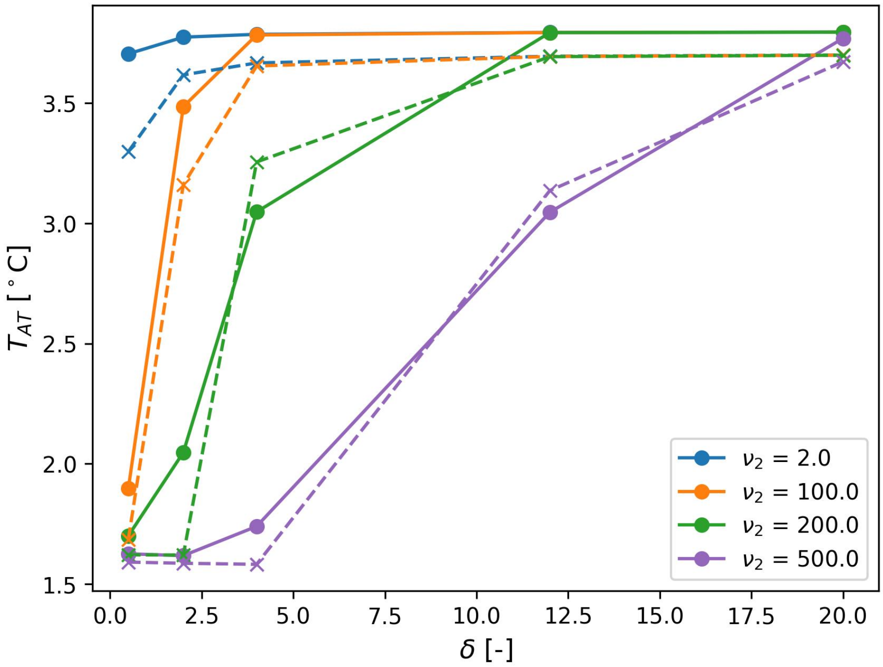

Figure 5.10: Atmospheric temperature after a model run of 80 years plotted against some values of δ ($\delta = 0.5, 2, 4, 12\text{and}20$).

Chapter 6

Discussion

This chapter discusses the results of the coupling of DICE-2023 (an ecological-economic model) with the social model of Maghsoodlo et al. [10] and how these results can contribute to further research. The choices for the coupling of the models are discussed as well.

Some results of the coupled model show high (larger than a 10 °C increase) atmospheric temperatures for the 2-timescale equilibrium. Examples of such results are for low values of κ in Figure 5.2, ν_2 in Figure 5.4 and $\Delta\mu_{max}$ in Figure 5.6. These high temperature increases do not correspond with current literature and prognoses of climate models for possible temperatures, but DICE is not designed to be used for simulations of thousands of years. However, the temperature model equations of DICE are calibrated up to a certain temperature. The equations of DICE are based on the FAIR model (Finite-amplitude Impulse Response model), which is calibrated to CMIP models up to temperature increases of 8°C in the paper of Smith et al. [38]. The Coupled Model Intercomparison Project (CMIP) combines multiple climate models describing physical processes and is used for the Intergovernmental Panel on Climate Change (IPCC) reports [39]. The atmospheric temperatures increases higher than 8 °C of this thesis should not be considered as accurate simulations, but rather as an indication that the state of the world is a worst-case scenario for humanity and the ecology on Earth.

The social part of the model only has two solutions for the fraction of mitigators x; $x = 0$ or $x = 1$. This model used one equation for the social part of the model, it may be that there are more stable solutions possible in reality. This reality with more stable solutions could be modelled with other more complex social models. These complex models might have more equations for the social dynamics or they consider the population to be divided into clusters with different parameter values. The results of the coupled model used in this research showed that different combinations of values of ν_2, δ and initial support x_0 are important for the trajectory of atmospheric temperature. This knowledge can contribute to the development of these more complex social models; the knowledge that select parameters are important is useful in a model with a large number of parameters that need to be investigated.

The used social model assumes a bifurcation in public support by design of the model equation. Probably, the model equation does not describe the real world with a high accuracy, as in reality more factors contribute to social dynamics. Additionally, this model assumes a uniform distribution of support levels across society, but in reality, the support for climate policy will differ between societal clusters. Even though this model is not highly realistic, it is probable that dynamics described by this model do happen in reality. The results show that the perceived weight of damage cost and strength of social norms are important for the dynamics. These factors could be influenced to improve support for climate policy.

The mitigation cost function is proportional to the level of mitigation as stated by the DICE model. This leads to the scenario where support increases to almost 1, but the maximum cost of this policy will be perceived in the next timestep (5 years later). In this scenario the mitigation cost, and with that the incentive to not support climate policy, only occurs when support is already at a high level from which society would not deviate. It could be interesting to change this coupling to a relation where mitigation costs depend on the rate of change of emissions control rate μ, rather than the value of μ itself. Probably, the process of switching from support levels would occur more slowly and might even oscillate. Eventually, the rising temperature due to this delay in climate policy, will shift the public opinion to support full mitigation from emissions.

The damage function only considers the current atmospheric temperature. With this damage function in the model, people would only take into account the current state of the world. In reality, policy makers and the public also consider future prospects. This could be reflected in the coupled model by using a discounted damage function, where future damages are taken into account as well. In that case, damages in the far future have a smaller weight than damages in the near future.

Chapter 7

Conclusions

For this research, an ecological-economic model is coupled with a social model to investigate the potential of public support for climate policy. The aim of this thesis is to determine how the coupling between atmospheric temperature and public support influences global warming in a coupled ecological-economic-social model. In particular, an interest of this research is the finding of tipping points that influence climate change in a positive or negative way.

The coupling of the public support with atmospheric temperature influences global warming in the coupled model in the following way. If public support for climate policy converges to a lower level for some period of time, this delay in climate policy implementation ensures a higher global warming. In the case that public support rises fairly quickly, the global warming stays in the desired limit of 2 °C. There are multiple factors into play that influence this behaviour and even the changing of one parameter can change the influence another parameter has. Some examples of factors that cause a delay in climate policy in certain parameter settings are: a low value of the perceived weight for the damage costs ν_2, social learning rate κ and maximum bound for the change in climate policy $\Delta\mu_{max}$.

The perceived cost balance of mitigation and damages ψ and the strength of the social norms δ determine the behaviour of the public support x in the social model. The significance of the relation between these variables can also be seen in the results for the coupled model. In the range $\psi \in [-\delta, \delta]$ there are two attraction domains for the solution $x = 0$ and $x = 1$. The initial value of x_0 and ψ determine in which attraction domain the model run starts and thus if the public support initially decreases (which result in high global warming) or not. The value of δ changes this range and therefore can change the influence of x_0 and ψ on the model run.

The perceived weight of the damage costs ν_2 is a factor in ψ. Small values of ν_2 lead to a strong global warming effect (as the simulation is placed in the attraction domain for no public support). Whereas larger values of ν_2 ensure that the temperature increase stays in a range around 2°C (the simulation is placed in the attraction domain for full public support). This influence is not the case for the perceived weight of mitigation costs ν_1. No influence of ν_1 on the global warming is found. This is because the mitigation costs rises when public support is already high. In that case, the higher mitigation costs do not have a strong impact on public support, as social norms will keep the public support for climate policy high. It is probable that this relation changes for other parameter values.

The social learning rate κ is the following; for low values of κ the temperature increase is high and for larger values the global warming stays around 2°C.
The coupling of the social model to DICE is characterized by the upper and lower limit in which policy parameter μ is allowed to change. The lower bound $\Delta\mu_{min}$ had a small influence; all global warming was around 2°C. This relation could be different in other parameter settings with a longer period of low support. The upper bound $\Delta\mu_{max}$ did have an influence; if the upper limit is too low, the temperature increase is high.

References

1. Sognnaes, I., Gambhir, A., van de Ven, D, Nikas, A., Anger-Kraavi, A., Bui, H., Campagnolo, L., Delpiazzo, E., Doukas, H., Giarola, S., et al. (2021). “A multi-model analysis of long-term emissions and warming implications of current mitigation efforts”. In: *Nature Climate Change* 11.12, pp. 1055–1062.

2. World Meteorological Organization (2026a). *State of the Global Climate 2025*. Tech. rep. WMO-No. 1391. WMO.

3. — (2026b). *Significant Weather Climate Events 2025*. Tech. rep. WMO.

4. Weart, Spencer R.. (2003). “The Discovery of Rapid Climate Change”. In: *Phyics Today*. DOI: 10.1063/1.1611350.

5. Luterbacher, U. and Sprinz, D. (2001). *International relations and global climate change*. MIT Press.

6. Nascimento, L., Kuramochi, T., Iacobuta, G., den Elzen, M., Fekete, H., Weishaupt, M., van Soest, H., Roelfsema, M., Vivero-Serrano, G., Lui, S., et al. (2022). “Twenty years of climate policy: G20 coverage and gaps”. In: *Climate policy* 22.2, pp. 158–174.

7. Nordhaus, W. (2018). “Evolution of modeling of the economics of global warming: changes in the DICE model, 1992–2017”. In: *Climatic change* 148.4, pp. 623–640.

8. Bastiaansen, R., Dijkstra, H., and von der Heydt, A. (2022). “Fragmented tipping in a spatially heterogeneous world”. In: *Environmental Research Letters* 17.4, p. 045006.

9. Krasnopolsky, V. and Fox-Rabinovitz, M. (2006). “Complex hybrid models combining deterministic and machine learning components for numerical climate modeling and weather prediction”. In: *Neural Networks* 19.2, pp. 122–134.

10. Babazadeh Maghsoodlo, Y., Anand, M., and Bauch, C. (2025). "Social dynamics can delay or prevent climate tipping points by speeding the adoption of climate change mitigation". In: *arXiv preprint*.

11. Moore, F., Lacasse, K., Mach, K., Shin, Y., Gross, L., and Beckage, B. (2022). "Determinants of emissions pathways in the coupled climate–social system". In: *Nature* 603.7899, pp. 103–111.

12. Bretter, C. and Schulz, F. (2025). "Public support for climate policies and its ideological predictors across countries of the Global North and Global South". In: *Ecological Economics* 233, p. 108603.

13. Constantino, S., Sparkman, G., Kraft-Todd, G., Bicchieri, C., Centola, D., Shell-Duncan, B., Vogt, S., and Weber, E. (2022). "Scaling up change: a critical review and practical guide to harnessing social norms for climate action". In: *Psychological science in the public interest* 23.2, pp. 50–97.

14. Parson, E. and Fisher-Vanden, K. (1997). "Integrated assessment models of global climate change". In: *Annual Review of Energy and the Environment* 22.1, pp. 589–628.

15. Pasqualino, R., Peñasco, C., Barbrook-Johnson, P., de Moura, F., Kolesnikov, S., Hafner, S., Nijsse, F., Lamperti, F., Hinder, B., Melekh, Y., et al. (2024). "Modelling induced innovation for the low-carbon energy transition: a menu of options". In: *Environmental Research Letters* 19.7, p. 073004.

16. Ikefuji, M., Laeven, R., Magnus, J., and Muris, C. (2021). "DICE simplified". In: *Environmental Modeling & Assessment* 26.1, pp. 1–12.

17. Cai, Y., Judd, K., and Lontzek, T. (2012). *Continuous-time methods for integrated assessment models*. Tech. rep. National Bureau of Economic Research.

18. Grubb, M., Wieners, C., and Yang, P. (2021). "Modeling myths: On DICE and dynamic realism in integrated assessment models of climate change mitigation". In: *Wiley Interdisciplinary Reviews: Climate Change* 12.3, e698.

19. Linsenmeier, M., Mohommad, A., and Schwerhoff, G. (2023). "Global benefits of the international diffusion of carbon pricing policies". In: *Nature Climate Change* 13.7, pp. 679–684.

20. Climate Change, Intergovernmental Panel of (2025). *About; IPCC — ipcc.ch*. `https://www.ipcc.ch/about/`. [Accessed 14-11-2025].

21. Biswas, P., Salazar, J., Kwakkel, J., and Marangoni, G. (2025). "Prioritizing the Welfare of Vulnerable Nations Promotes Equitable Achievement of Paris Target". In.

22. Kanitkar, T., Mythri, A., and Jayaraman, T. (2024). "Equity assessment of global mitigation pathways in the IPCC Sixth Assessment Report". In: *Climate Policy* 24.8, pp. 1129–1148.

23. De Marchi, S. and Page, S. (2014). "Agent-based models". In: *Annual Review of political science* 17.1, pp. 1–20.

24. Lamperti, F., Dosi, G., Napoletano, M., Roventini, A., and Sapio, A. (2018). "Faraway, so close: coupled climate and economic dynamics in an agent-based integrated assessment model". In: *Ecological Economics* 150, pp. 315–339.

25. van Nes, E., Arani, B., Staal, A., van der Bolt, B., Flores, B., Bathiany, S., and Scheffer, M. (2016). "What do you mean,'tipping point'?" In: *Trends in ecology & evolution* 31.12, pp. 902–904.

26. Milkoreit, M., Hodbod, J., Baggio, J., Benessaiah, K., Calderón-Contreras, R., Donges, J., Mathias, J., Rocha, J., Schoon, M., and Werners, S. (2018). "Defining tipping points for social-ecological systems scholarship—an interdisciplinary literature review". In: *Environmental Research Letters* 13.3, p. 033005.

27. Ashwin, P., Wieczorek, S., Vitolo, R., and Cox, P. (2012). "Tipping points in open systems: bifurcation, noise-induced and rate-dependent examples in the climate system". In: *Philosophical Transactions of the Royal Society A: Mathematical, Physical and Engineering Sciences* 370.1962, pp. 1166–1184.

28. Lenton, T. (2013). "Environmental tipping points". In: *Annual review of Environment and Resources* 38.1, pp. 1–29.

29. Seydel, Rüdiger (2009). *Practical Bifurcation and Stability Analysis*. Vol. 5. Springer, p. 57. ISBN: ISBN 978-1-4614-2530-4.

30. Barrage, L. and Nordhaus, W. (2024). "Policies, projections, and the social cost of carbon: Results from the DICE-2023 model". In: *Proceedings of the National Academy of Sciences* 121.13, e2312030121.

31. Barrage, L. and Nordhaus, W. (2023a). *Supplemental Materials: Statistical and Methods Appendices to the DICE-2023 Model*.

32. Mankiw, N. (2019). *Macroeconomics*. Worth Publishers.

33. Welch, I. (n.d.). *DICE 2023 — ivo-welch.info*. `https://www.ivo-welch.info/research/dice/header.html`. [Accessed 09-12-2025].

34. Barrage, L. and Nordhaus, W. (2023b). *Background Note on DFAIR*. `https://yale.app.box.com/s/whlqcr7gtzdm4nxnrfhvap2hlzebuvvm/file/1264784735138`. [Accessed 16-06-2026], "Background notes are for informational purposes and are not published.".

35. Nordhaus, W. (2007). *The challenge of global warming: economic models and environmental policy*. Vol. 4. Citeseer.

36. Bury, T., Bauch, C., and Anand, M. (2019). "Charting pathways to climate change mitigation in a coupled socio-climate model". In: *PLoS computational biology* 15.6, e1007000.

37. Wiggins, Stephen (2003). *Introduction to applied nonlinear dynamical systems and chaos*. Springer, pp. 366–370.

38. Smith, C., Cummins, D., Fredriksen, H., Nicholls, Z., Meinshausen, M., Allen, M., Jenkins, S., Leach, N., Mathison, C., and Partanen, A. (2024). "fair-calibrate v1. 4.1: calibration, constraining, and validation of the FaIR simple climate model for reliable future climate projections". In: *Geoscientific Model Development* 17.23, pp. 8569–8592.

39. World Meteorological Organization (2023). *Climate Projections in Next Phase of the Coupled Model Intercomparison Project*. Bulletin Vol. 72 (2) - 2023.

Appendices

Appendix A

Exogenous variables

In chapter 3.1 the DICE model is explained. In this appendix the exogenous variables, parameter values and initial conditions are given.

$$
\begin{aligned}
L[t_{i+1}]) &= L[t_i]\left(\frac{10825}{L[t_i]}\right)^{0.145} \\
L[t_0] &= 7752.9
\end{aligned}
\tag{A.1}
$$

$$
\begin{aligned}
A[t_{i+1}] &= \frac{A[t_i]}{1-0.066e^{-0.0015t_i}} \\
A[t_0] &= 5.84
\end{aligned}
\tag{A.2}
$$

$$
r_\sigma[t_i] = -0.015 \cdot 0.96^i \tag{A.3}
$$

$$
\begin{aligned}
\sigma[t_{i+1}] &= \sigma[t_i]e^{r_\sigma[t_i]\Delta t} \\
\sigma[t_0] &= \frac{E[t_0]}{Q[t_0](1-\mu[t_0])}
\end{aligned}
\tag{A.4}
$$

$$
\theta_1[t_i] = 515 r_\sigma[t_i]\sigma[t_i] \cdot \begin{cases} e^{-0.01\Delta t(i-6)}, i < 7 \\ e^{-0.001\Delta t(i-6)}, i \geq 7 \end{cases} \tag{A.5}
$$

$$
E_{land}[t_i] = 5.9 \cdot 0.9^i \tag{A.6}
$$

$$
E_{abate}[t_i] = \begin{cases} 9.96 + \frac{i}{16}(15.5-9.96), & i < 16 \\ 15.5, & i \geq 16 \end{cases} \tag{A.7}
$$

Table A.1: Parameter values and initial conditions used in the DICE model

Variable	Value	Unit
γ	0.300	-
δ_k	0.100	yr^{-1}
$Q[t_0]$	135.7	trill 2019 USD
$E[t_0]$	37.56	GtCO2/y
$\mu[t_0]$	0.05	
ψ_1	0.0	-
ψ_2	0.003467	-
θ_1	0.109062	
θ_2	2.6	-
ξ_0	0.2173	-
ξ_1	0.224	-
ξ_2	0.2824	-
ξ_3	0.2763	-
τ_0	1000000	y
τ_1	394.4	y
τ_2	36.53	y
τ_3	4.304	y
ζ_0	32.4	y
ζ_C	0.019	y/GtC
ζ_T	4.165	y/K
η	3.93	W/m^2

$$F_{EX}[t_i] = \begin{cases} -0.054 + \frac{i}{16}(0.265 + 0.054), & i < 16 \\ 0.265, & i \geq 16 \end{cases} \tag{A.8}$$

Appendix B

Extra explanation on model equations

B.1 Adaptation of the carbon reservoir equation

In this section we will derive the other equation (3.8) for the carbon reservoir, from equation 3.7;

$$\Delta R_j(t+1) = \xi_i E_{CO_2}(t) - \frac{R_j(t)}{\alpha(t)\tau_i}. \qquad i = 1,2,3,4. \tag{B.1}$$

We translate the difference equation to a differential equation by taking the limit $\Delta t \to 0$,

$$\frac{dR_j}{dt}(t) = \xi_i E_{CO_2}(t) - \frac{R_j(t)}{\alpha(t)\tau_i} \tag{B.2}$$

The homogeneous solution of this differential equation is,

$$R_{j\,hom}(t) = C_1 e^{-\int_{t_0}^{t} \frac{1}{\tau_i \alpha(\tilde{t})} d\tilde{t}}. \tag{B.3}$$

Using the method of variation of parameters we find a general expression for the particular solution,

$$R_{j\,part}(t) = C_1(t) e^{-\int_{t_0}^{t} \frac{1}{\tau_i \alpha(\tilde{t})} d\tilde{t}}. \tag{B.4}$$

Substitution of the particular solution (B.4) into the differential equation B.2, leads to,

$$\frac{dC_1(t)}{dt} e^{-\int_{t_0}^{t} \frac{1}{\tau_i \alpha(\tilde{t})} d\tilde{t}} - \frac{1}{\tau_i \alpha(t)} C_1(t) e^{-\int_{t_0}^{t} \frac{1}{\tau_i \alpha(\tilde{t})} d\tilde{t}} = \xi_i E_{CO_2}(t) - \frac{R_j(t)}{\tau_i \alpha(t)}. \tag{B.5}$$

This simplifies to,

$$\frac{dC_1(t)}{dt} = \xi_i E_{CO_2}(t) e^{\int_{t_0}^{t} \frac{1}{\tau_i \alpha(\tilde{t})} d\tilde{t}}. \tag{B.6}$$

In the case that $t - t_0$ is sufficiently small,

$$\int_{t_0}^{t} \frac{1}{\tau_i \alpha(\tilde{t})} d\tilde{t} \approx \frac{t - t_0}{\tau_i \alpha(t)}. \tag{B.7}$$

From integrating equation B.6, we find an expression for $C_1(t)$,

$$C_1(t) = \int_{t_0}^{t} \xi_i E_{CO_2}(\tilde{t}) e^{\frac{\tilde{t}-t_0}{\tau_i \alpha(\tilde{t})}} d\tilde{t} + C_2. \tag{B.8}$$

Which will be used for finding the particular solution,

$$\begin{aligned} R_{jpart}(t) &= \int_{t_0}^{t} \xi_i E_{CO_2}(\tilde{t}) e^{\frac{\tilde{t}-t_0}{\tau_i \alpha(\tilde{t})}} d\tilde{t} e^{-\frac{t-t_0}{\tau_i \alpha(t)}} && \text{(B.9)} \\ &\approx \xi_i E_{CO_2}(\tilde{t}) \tau_i \alpha(\tilde{t}) e^{\frac{\tilde{t}-t_0}{\tau_i \alpha(\tilde{t})}} \Bigg|_{t_0}^{t} e^{-\frac{t-t_0}{\tau_i \alpha(t)}} && \text{(B.10)} \\ &\approx \xi_i E_{CO_2}(t) \tau_i \alpha(t) \left(1 - e^{-\frac{t-t_0}{\tau_i \alpha(t)}}\right). && \text{(B.11)} \end{aligned}$$

As the term with C_2 represents the homogeneous solution, it is left out in equation B.9 and will be included in the general solution. For the approximation of the integral in equation B.10, it is assumed that t is sufficiently close to t_0 and the evaluation of E_{CO_2} and α on t and t_0 are close as well.

The general solution becomes,

$$R_j(t) = \xi_i E_{CO_2}(t) \tau_i \alpha(t) \left(1 - e^{-\frac{t-t_0}{\tau_i \alpha(t)}}\right) + C_2 e^{-\frac{t-t_0}{\tau_i \alpha(t)}}. \tag{B.12}$$

Using the initial condition this results in,

$$R_j(t) = \xi_i E_{CO_2}(t) \tau_i \alpha(t) \left(1 - e^{-\frac{t-t_0}{\tau_i \alpha(t)}}\right) + R_j(t_0) e^{-\frac{t-t_0}{\tau_i \alpha(t)}}. \tag{B.13}$$

B.2 Relation E_{CO_2} and α

Section 3.1.4.1 states a positive correlation between the carbon emissions E_{CO_2} and saturation parameter α. This follows from the results shown in Figure B.1. To generate these results, the DICE model was run for 100 years with μ a hyperbolic tangent with $t_\mu = 200$ years. The variable values after this run, together with a fixed value of E_{CO_2}, were used as input for the calculation of α.

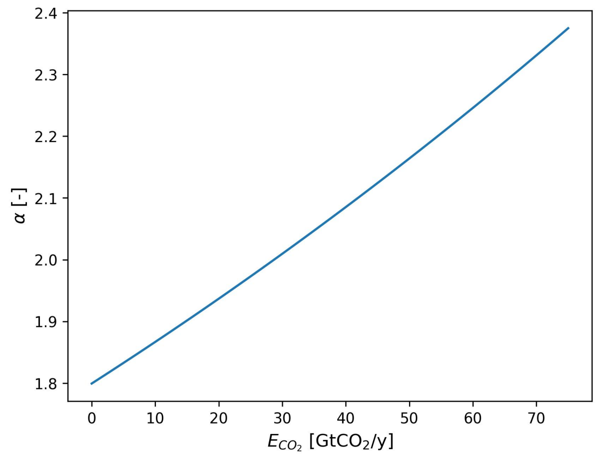

Figure B.1: Relation between saturation parameter α and carbon emissions E_{CO_2} in DICE-2023. The model was first run for 100 years with μ a hyperbolic tangent with $t_\mu = 200$ years. The model variables after this model run were used as input of the function for α to determine the relation.

B.3 Derivation of 2-timescale model equations

In this section the derivation of the new system of equations with use of the 2-timescale method is continued from section 3.1.4.2. We will introduce a new constant ϵ_1 for notation purposes,

$$\epsilon_1 := \frac{e^{-5/236} - 1}{\Delta t}. \tag{B.14}$$

The differential equation for T_1 follows in a similar way as in section 3.1.4.2,

$$\frac{\partial T_1^0}{\partial t}(t,\tau) + \epsilon \frac{\partial T_1^0}{\partial \tau}(t,\tau) + \frac{\partial T_1^1}{\partial t}(t,\tau) + \epsilon \frac{\partial T_1^1}{\partial \tau}(t,\tau) + \cdots = -\epsilon_1 (T_1^0 + T_1^1 + \dots) + 0.324\epsilon_1 (F^0 + F^1 + \dots). \tag{B.15}$$

The leading equation of this expanded differential equation is,

$$\frac{\partial T_1^0}{\partial t}(t,\tau) = 0. \tag{B.16}$$

The same approach is used for finding an expression for T_2. An important difference between the differential equations of T_1 and T_2 is the order of the exponential ($\mathcal{O}(\epsilon)$ and $\mathcal{O}(1)$, respectively).

$$\begin{aligned}
&\frac{\partial T_2^0}{\partial t} + \epsilon \frac{\partial T_2^0}{\partial \tau} + \frac{\partial T_2^1}{\partial t} + \epsilon \frac{\partial T_2^1}{\partial \tau} + \dots \\
&\qquad\qquad = (T_2^0 + T_2^1 + \dots)\frac{1}{\Delta t}\left(e^{-\Delta t/4.07} - 1\right) \\
&\qquad\qquad + 0.44(F^0 + F^1 + \dots)\frac{1}{\Delta t}\left(1 - e^{-\Delta t/4.07}\right)
\end{aligned} \tag{B.17}$$

From the leading equation, an expression for T_2 follows.

$$\frac{\partial T_2^0}{\partial t} = T_2^0 \frac{1}{\Delta t}\left(e^{-\Delta t/4.07} - 1\right) + 0.44F^0\frac{1}{\Delta t}\left(1 - e^{-\Delta t/4.07}\right) \tag{B.18}$$

This finishes the analysis of order expansion for the differential equations. We continue with the algebraic equations as these are also influenced by the order expansion.

$$\begin{aligned}
&M_{AT}^0 + M_{AT}^1 + M_{AT}^2 + \dots \\
&\qquad = (R_1^0 + R_1^1 + \dots) + (R_2^0 + R_2^1 + \dots) + (R_3^0 + R_3^1 + \dots) \\
&\qquad + (R_4^0 + R_4^1 + \dots) + M_{AT}(1765)
\end{aligned} \tag{B.19}$$

The leading equation is,

$$M_{AT}^0(\tau) = R_1^0(\tau) + R_2^0(\tau) + R_3^0(\tau) + R_4^0(\tau) + M_{AT}(1765). \tag{B.20}$$

Substitution of $M_{AT}^0(\tau)$ in the equation for accumulated carbon yields,

$$C_{acc}(\tau) = C_{tot} - (M_{AT}^0(\tau) - M_{AT}(1765)). \tag{B.21}$$

In order to find the leading equation for the radiative forcing, we take the Taylor expansion of M_{AT} around M_{AT}^0 with the introduction of $\Delta M_{AT}(t,\tau) := M_{AT}(t,\tau) - M_{AT}^0(\tau)$.

$$M_{AT} = M_{AT}^0 + \left.\frac{\partial M_{AT}}{\partial M_{AT}^0}\right|_{M_{AT}^0} \Delta M_{AT} + \frac{1}{2}\left.\frac{\partial^2 M_{AT}}{(\partial M_{AT}^0)^2}\right|_{M_{AT}^0} (\Delta M_{AT})^2 + \dots \tag{B.22}$$

Realizing that the derivative with respect to M_{AT}^0 is 1, simplifies the Taylor expansion.

$$M_{AT} = M_{AT}^0 + \Delta M_{AT} + \frac{1}{2}\left(\Delta M_{AT}\right)^2 + \dots \tag{B.23}$$

The order expanded expression for the radiative forcing is,

$$\begin{aligned} F^0 + F^1 + \dots &= \eta \log_2\left(\frac{M_{AT}^0 + \Delta M_{AT} + \frac{1}{2}\left(\Delta M_{AT}\right)^2 + \dots}{M_{AT}(1765)}\right) + F_{EX} \\ &= \eta \log_2\left(\frac{M_{AT}^0}{M_{AT}(1765)}\right) + \eta \log_2\left(\frac{1 + \Delta M_{AT} + \frac{1}{2}\left(\Delta M_{AT}\right)^2 + \dots}{M_{AT}^0}\right) + F_{EX}. \end{aligned} \tag{B.24}$$

From this we extract the leading equation,

$$F^0(\tau) = F_{EX} + \eta \log_2\left(\frac{M_{AT}^0(\tau)}{M_{AT}(1765)}\right). \tag{B.25}$$

The leading equation for T_{AT} is straightforwardly defined by,

$$T_{AT}^0 = T_1^0 + T_2^0. \tag{B.26}$$

The last equation for which the two-timescale method needs to be applied is the implicit expression for α.

$$\zeta_0 + \zeta_C\left(C_{acc}^0 + C_{acc}^1 + \dots\right) + \zeta_T(T_{AT}^0 + T_{AT}^1 + \dots) = \sum_{i=1}^{4}(\alpha^0 + \alpha^1 + \dots)\xi_i\tau_i\left(1 - e^{-\frac{100}{(\alpha^0+\alpha^1+\dots)\tau_i}}\right) \tag{B.27}$$

As stated earlier τ_1 and τ_2 are $\mathcal{O}(\epsilon)$ and τ_3 and τ_4 $\mathcal{O}(1)$, the threshold between the two timescales lays around $\frac{1}{200}$. Assuming the value of α does not impact the order, the exponential term is $\mathcal{O}(1)$ for $i = 1, 2, 3$. We investigate the order expansion of α with a Taylor expansion.

$$e^{-\frac{100}{(\alpha^0+\Delta\alpha)\tau_i}} \approx e^{-\frac{100}{\alpha^0\tau_i}} + \frac{100}{(\alpha^0)^2\tau_i}e^{-\frac{100}{\alpha^0\tau_i}}\Delta\alpha + \dots \tag{B.28}$$

The second term is $\mathcal{O}(\epsilon)$ due to $\Delta\alpha$. The leading equation is,

$$\zeta_0 + \zeta_C C_{acc}^0 + \zeta_T T_{AT}^0 = \sum_{i=1}^{3}\alpha^0\xi_i\tau_i\left(1 - e^{-\frac{100}{\alpha^0\tau_i}}\right) + \alpha^0\xi_4\tau_4. \tag{B.29}$$

Appendix C

Code

C.1 DICE-2023 model

```python
### Import ###
import numpy as np
import matplotlib.pyplot as plt
from dataclasses import dataclass
import copy
import random
import math
import scipy.optimize
from Log_v1 import *

#define hyperbolic tangent and linear functions for mu
def mu_tanh(n, dt, T_mu):
    i_T = int(T_mu/dt)
    mu0 = 0.049999999
    arc = np.arctanh(2*mu0-1)
    b = T_mu/(np.pi-arc)
    mu = np.ones(n)
    if i_T>=n:
        mu = 0.5+0.5*np.tanh((np.arange(0, n)*dt+b*arc)/b)
        return mu
    mu[:i_T+1] = 0.5+0.5*np.tanh((np.arange(0, i_T+1)*dt+b*arc)/b)
    return mu

def mu_lin(n, dt, T_mu):
```

```
    i_T = int(T_mu/dt)
    mu0 = 0.04999999
    mu = np.ones(n)
    if i_T>=n:
        mu = (1-mu0)/T_mu*np.arange(0, n)*dt + mu0
        return mu
    mu[:i_T+1] = (1-mu0)/T_mu*np.arange(0, i_T+1)*dt + mu0
    return mu


### Parameters ###
@dataclass
class Param:
    sigma: list = 0                     #ratio output to emissions
    E_land: list = 0                    #emissions from land
    eta: float = 0                      #temperature-forcing
    F_EX: list = 0                      #exogenous radiative forcing
    F_EXlim: float = 0                  #exogenous radiative forcing limit
    E_nonCO2aba: list = 0
    M_AT0: float = 0                    #initial carbon in atmosphere in 1765
    tau: list = 0                       #delays of carbon reservoirs
    xi: list = 0
    zeta: list = 0                      #coefficients
    psi2: float = 0                     #parameter for damage function
    theta1: list = 0                    #parameters abatement cost
    theta2: float = 0                   #parameters abatement cost
    L: list = 0                         #labour
    A: list = 0                         #productivity factor
    gamma: float = 0                    #capital's share of income
    epsilon_k: float = 0                #depreciation rate
      ### different from delt_K from Nordhaus ###
    r: float = 0                        #investment rate

### Variables ###

#Class for storing and calculating the variables of DICE in a timestep
@dataclass
class World:
    i: int = 0
```

```
    E_CO2: float = 0                #CO2 emissions
    alpha: float = 0
    C_tot: float = 0
    F_aba: float = 0
    F: float = 0                    #total radiative forcing
    T1: float = 0                   #temperature box 1
    T2: float = 0                   #temperature box 2
    T_AT: float = 0
    R0: float = 0
    R1: float = 0
    R2: float = 0
    R3: float = 0
    M_AT: float = 0
    C_acc: float = 0
    iRF100: float = 0
    Omega: float = 0                #damage function
    Lambda: float = 0               #abatement cost
    K: float = 0                    #kapital
    I: float = 0                    #investment
    O: float = 0                    #output
    Q: float = 0                    #global product

   #scipy.optimize.root(alpha_impl, guess, method = "hybr")

    #Timestep in DICE
    def timestep(self, par, dt, mu1, mu):
        #implicit function to find alpha
        def alpha_impl(alpha, dt, R_old, E_CO2, E_CO2_old, Ctot, T1, T2,
                                F_aba, F_EX, zeta, xi, tau, eta, M_AT0):
            e0      = np.exp(-dt/(tau[0]*alpha))
            R0      = xi[0]*tau[0]*alpha*E_CO2/3.667*(1-e0)+R_old[0]*e0
            e1      = np.exp(-dt/(tau[1]*alpha))
            R1      = xi[1]*tau[1]*alpha*E_CO2/3.667*(1-e1)+R_old[1]*e1
            e2      = np.exp(-dt/(tau[2]*alpha))
            R2      = xi[2]*tau[2]*alpha*E_CO2/3.667*(1-e2)+R_old[2]*e2
            e3      = np.exp(-dt/(tau[3]*alpha))
            R3      = xi[3]*tau[3]*alpha*E_CO2/3.667*(1-e3)+R_old[3]*e3
            Cacc    = Ctot-(R0+R1+R2+R3)+E_CO2_old*dt/3.666
            M_AT    = R0+R1+R2+R3+M_AT0
```

```
            LHS      = alpha*(xi[0]*tau[0]*(1-np.exp(-100/alpha/tau[0]))
                              +xi[1]*tau[1]*(1-np.exp(-100/alpha/tau[1]))
                              +xi[2]*tau[2]*(1-np.exp(-100/alpha/tau[2]))
                              +xi[3]*tau[3]*(1-np.exp(-100/alpha/tau[3])))
            F        = eta*np.log(M_AT/M_AT0)/np.log(2)+F_aba+F_EX
            T1       = T1*np.exp(-5/236)+0.324*F*(1-np.exp(-5/236))
            T2       = T2*np.exp(-5/4.07)+0.44*F*(1-np.exp(-5/4.07))
            T_AT     = T1+T2
            RHS      = zeta[0]+zeta[1]*Cacc+zeta[2]*T_AT
            return LHS-RHS

        #Update economy variables
        new = copy.deepcopy(self)
        new.i += 1
        new.K = (1-par.epsilon_k)**dt*self.K+dt*self.I
        new.O = par.A[new.i]*new.K**par.gamma
            *(par.L[new.i]/1000)**(1-par.gamma)

        #Update ecology variables
        new.E_CO2 = (par.sigma[new.i]*new.O + par.E_land[new.i])*(1-mu)
        new.F_aba = 0.861*self.F_aba+0.00955*par.E_nonCO2aba[new.i-1]*(1-mu1)

        #define implicit function alpha with current values
        fun = lambda x: alpha_impl(x, dt, [self.R0, self.R1, self.R2, self.R3],
                            new.E_CO2, self.E_CO2, self.C_tot, self.T1, self.T2,
                            new.F_aba, par.F_EX[new.i], par.zeta, par.xi,
                            par.tau, par.eta, par.M_AT0)

        #find alpha
        result      = scipy.optimize.root(fun, self.alpha, method="hybr")
        new.alpha   = result.x[0]

        #update ecology variables
        e0          = np.exp(-dt/par.tau[0]/new.alpha)
        new.R0      = par.xi[0]*par.tau[0]*new.alpha*new.E_CO2/3.667*(1-e0)
                                                                    +self.R0*e0
        e1          = np.exp(-dt/par.tau[1]/new.alpha)
        new.R1      = par.xi[1]*par.tau[1]*new.alpha*new.E_CO2/3.667*(1-e1)
                                                                    +self.R1*e1
```

```
        e2          = np.exp(-dt/par.tau[2]/new.alpha)
        new.R2      = par.xi[2]*par.tau[2]*new.alpha*new.E_CO2/3.667*(1-e2)
                                                                +self.R2*e2
        e3          = np.exp(-dt/par.tau[3]/new.alpha)
        new.R3      = par.xi[3]*par.tau[3]*new.alpha*new.E_CO2/3.667*(1-e3)
                                                                +self.R3*e3
        new.M_AT    = new.R0+new.R1+new.R2+new.R3+par.M_AT0
        new.F       = par.eta*np.log(new.M_AT/par.M_AT0)/np.log(2)
                                              +new.F_aba+par.F_EX[new.i]
        new.C_tot   = self.C_tot + self.E_CO2*dt/3.666
        new.C_acc   = new.C_tot - new.M_AT + par.M_AT0
        new.T1      = self.T1*np.exp(-5/236)+0.324*new.F*(1-np.exp(-5/236))
        new.T2      = self.T2*np.exp(-5/4.07)+0.44*new.F*(1-np.exp(-5/4.07))
        new.T_AT    = new.T1+new.T2
        new.iRF100  = par.zeta[0]+par.zeta[1]*new.C_acc+par.zeta[2]*new.T_AT

        #update the money flows
        new.Lambda  = par.theta1[new.i]*mu**par.theta2
        new.Omega   = par.psi2*new.T_AT**2
        new.Q       = max(0, (1-new.Omega-new.Lambda)*new.O)
        new.I       = par.r*new.Q
        return new

#Class for calculating the equilibrium
@dataclass
class Eco:
    R0:     float = 0
    R1:     float = 0
    R2:     float = 0
    R3:     float = 0
    M_AT:   float = 0
    C_acc:  float = 0
    alpha:  float = 0
    F:      float = 0
    T1:     float = 0
    T2:     float = 0
    T_AT:   float = 0

    def __init__(self, world):
```

```
        self.R0      = world.R0
        self.R1      = world.R1
        self.R2      = world.R2
        self.R3      = world.R3
        self.M_AT    = world.M_AT
        self.C_acc   = world.C_acc
        self.alpha   = world.alpha
        self.F       = world.F
        self.T1      = world.T1
        self.T2      = world.T2
        self.T_AT    = world.T_AT
        self.C_tot   = world.C_tot

    def update(self, dx):
        self.R0      += dx[0][0]
        self.R1      += dx[1][0]
        self.R2      += dx[2][0]
        self.R3      += dx[3][0]
        self.M_AT    += dx[4][0]
        self.M_AT = max(self.M_AT, 10E-16)
        self.C_acc   += dx[5][0]
        self.alpha   += dx[6][0]
        self.F       += dx[7][0]
        self.T1      += dx[8][0]
        self.T2      += dx[9][0]
        self.T_AT    += dx[10][0]
        return self

    def func(self, par):
        f = np.zeros((11,1))
        R = [self.R0, self.R1, self.R2, self.R3]
        for i in range(4):
            f[i] = -R[i]/(self.alpha*par.tau[i])
            f[6] += self.alpha*par.xi[i]*par.tau[i]
                        *(1-np.exp(-100/(self.alpha*par.tau[i])))
        f[4]     = sum(R) - self.M_AT + par.M_AT0
        f[5]     = -self.C_acc + self.C_tot - self.M_AT + par.M_AT0
        f[6]    += -(par.zeta[0]+par.zeta[1]*self.C_acc+par.zeta[2]*self.T_AT)
        f[7]     = -self.F + par.eta*np.log(self.M_AT/par.M_AT0)/np.log(2)
```

```
                        + par.F_EXlim
        et1     = np.exp(-5/236)
        et2     = np.exp(-5/4.07)
        f[8]    = self.T1*(et1-1) + 0.324*self.F*(1-et1)
        f[9]    = self.T2*(et2-1) + 0.44*self.F*(1-et2)
        f[10]   = -self.T_AT + self.T1 + self.T2
        return f

    def jac(self, par):
        J = np.zeros((11, 11))
        R = [self.R0, self.R1, self.R2, self.R3]
        for i in range(4):
            J[i,i] = -1./(self.alpha*par.tau[i])
            J[i,6] = -R[i]/par.tau[i]
            J[4,i] = 1.
            J[6,6] += par.xi[i]*par.tau[i]*(1+(100/(self.alpha*par.tau[i])-1)
                                        *np.exp(-100/(self.alpha*par.tau[i])))
        J[4,4] = -1.
        J[5,4] = -1.
        J[5,5] = -1.
        J[5,10] = -par.zeta[2]
        J[6,5] = -par.zeta[1]
        J[6,10] = -par.zeta[2]
        J[7,4] = par.eta*par.M_AT0/(np.log(2)*self.M_AT)
        J[7,7] = -1.
        J[8,7] = 0.324*(1-np.exp(-5/236))
        J[9,7] = 0.44*(1-np.exp(-5/4.07))
        J[8,8] = np.exp(-5/236)-1.
        J[9,9] = np.exp(-5/4.07)-1.
        J[10,8] = 1.
        J[10,9] = 1.
        J[10,10] = -1.
        return J

    def nr(self, par, a = 1., e = 10**(-10)):
        error = np.max(np.abs(self.func(par)))
        while error>e:
            dx = np.linalg.solve(self.jac(par), -self.func(par))
            self = self.update(a*dx)
```

```
            error = np.max(np.abs(self.func(par)))
        return(self)

def initialize(n, dt):
    ### initialize parameters object ###
    p = Param()
    p.E_land = 5.9*0.9**np.arange(n)
    p.eta = 3.93
    p.F_EXlim = 0.265
    p.F_EX = np.full(n, 0.265)
    p.F_EX[:16] = -0.054 + 1/16.*(0.265+0.054)*np.arange(n)[:16]
    p.E_nonCO2aba = np.full(n, 15.5)
    p.E_nonCO2aba[:16] = 9.96 + 1/16.*(15.5-9.96)*np.arange(n)[:16]
    p.M_AT0 = 588.
    p.tau = list([1000000., 394.4, 36.53, 4.304])
    p.xi = list([0.2173, 0.224, 0.2824, 0.2763])
    p.zeta = list([32.4, 0.019, 4.165])
    p.psi2 = 0.003467
    p.theta2 = 2.6
    p.gamma = 0.3
    p.epsilon_k = 0.100
    p.r = 0.28

    #Functions for theta1
    theta1 = np.empty(n)
    theta1[:7] = 515.*np.exp(-0.01*dt*(np.arange(n)[:7]-6))/(1000*p.theta2)
    theta1[7:] = 515.*np.exp(-0.001*dt*(np.arange(n)[7:]-6))/(1000*p.theta2)
    emisrate = np.full(n, 1.40)
    emisrate[:16] += 1/16*(1.21-1.40)*np.arange(16)
    emisrate[16:] = 1.21

    #Set variables for recursive parameter functions
    E0 = 37.56
    Q0 = 135.7
    mu0 = 0.0499999999999
    sigma = np.empty(n)
    sigma[0] = E0/(Q0*(1-mu0))
    r_sigma = -0.015*0.96**np.arange(n)
    r_sigma[np.where(r_sigma>-0.005)]=-0.005
```

```
    L = np.empty(n)
    L[0] = 7752.9
    A = np.empty(n)
    A[0] = 5.84

    for i in range(1,n):
        sigma[i]=sigma[i-1]*np.exp(r_sigma[i-1]*dt)
        L[i] = L[i-1]*(10825/L[i-1])**0.145
        A[i] = A[i-1]/(1-0.066*np.exp(-0.0015*dt*(i-1)))

    p.theta1 = theta1*emisrate*sigma
    p.L = L
    p.A = A
    p.sigma = sigma

    ### initialize world object ###
    s = World()
    s.E_CO2 =  42.941200100526      #this is not the same value as used earlier
    s.F_aba = 0.518
    #s.F
    s.alpha = 0.3
    s.T1 = 0.1477
    s.T2 = 1.099454
    s.T_AT = s.T1 + s.T2
    s.R0 = 150.093
    s.R1 = 102.698
    s.R2 = 39.534
    s.R3 = 6.1865
    #s.M_AT
    #s.C_acc
    s.C_tot = 633.5
    #s.iRF100
    s.Omega = p.psi2*s.T_AT**2
    s.Lambda = p.theta1[0]*mu0**p.theta2
    s.K = 295.
    s.Q = 134.157937530958          #this is not the same value as used earlier
    s.I = p.r*s.Q
    return p, s
```

C.2 2-timescale method equilibrium

```
import numpy as np
from dataclasses import dataclass
from Log_v2 import *
import scipy.optimize

#Class similar to 'World' for ecological variables and finding equilibrium
@dataclass
class Eco_eq2t:
    R0:         float = 0
    R1:         float = 0
    R2:         float = 0
    R3:         float = 0
    M_AT:       float = 0
    C_acc:      float = 0
    alpha:      float = 0
    F:          float = 0
    T1:         float = 0
    T2:         float = 0
    T_AT:       float = 0
    epsilon:    float = 0.0005

    #calculate equilibrium from World object
    def __init__(self, world, par):
        self.R0     = world.R0
        self.R1     = world.R1
        self.R2     = 0.
        self.R3     = 0.
        self.M_AT   = self.R0 + self.R1 + par.M_AT0
        self.C_tot  = world.C_tot
        self.C_acc  = self.C_tot - (self.M_AT - par.M_AT0)
        self.F      = par.F_EX[-1]
                + par.eta*np.log(self.M_AT/par.M_AT0)/np.log(2)
        self.T1     = world.T1
        self.T2     = 0.44*self.F
        self.T_AT   = self.T1 + self.T2
        self.alpha  = world.alpha

        def alpha_impl(alpha, xi, tau, zeta, Cacc, T_AT):
```

```
            LHS      = alpha*(xi[0]*tau[0]*(1-np.exp(-100/(alpha*tau[0])))
                             +xi[1]*tau[1]*(1-np.exp(-100/(alpha*tau[1])))
                              +xi[2]*tau[2]*(1-np.exp(-100/(alpha*tau[2])))
                              +xi[3]*tau[3])
            RHS      = zeta[0]+zeta[1]*Cacc+zeta[2]*T_AT
            return LHS-RHS

        fun          = lambda x: alpha_impl(x, par.xi, par.tau, par.zeta,
                                                      self.C_acc, self.T_AT)
        result       = scipy.optimize.root(fun, 0.3, method = "hybr")
        if not result.success:
            print("Not found a value for alpha")
        self.alpha    = result.x[0]

    def func(self, par, dt, T1):
        f            = np.zeros((9,1))
        f[0]         = -1/(self.alpha*par.tau[2]*dt)*self.R2
        f[1]         = -1/(self.alpha*par.tau[3]*dt)*self.R3
        f[2]         = -self.T1 + T1
        et2          = np.exp(-dt/4.07)
        f[3]         = self.T2/dt*(et2-1)    + 0.44/dt*self.F*(1-et2)
        f[4]         = self.R0 + self.R1 - self.M_AT + par.M_AT0
        f[5]         = -self.C_acc + self.C_tot - self.M_AT + par.M_AT0
        f[6]         = -self.F + par.eta*np.log(self.M_AT/par.M_AT0)/np.log(2)
                                                                  + par.F_EX[-1]
        f[7]         = -self.T_AT + self.T1 + self.T2
        f[8]         = -(par.zeta[0]+par.zeta[1]*self.C_acc
                     +par.zeta[2]*self.T_AT) + self.alpha*par.xi[3]*par.tau[3]
        for i in range(3):
            f[8]   += self.alpha*par.xi[i]*par.tau[i]
                                   *(1-np.exp(-100/(self.alpha*par.tau[i])))
        return f
```

C.3 Logbook class

```
import numpy as np
import matplotlib.pyplot as plt
from dataclasses import dataclass
import math
```

```python

@dataclass
class Log:
    att: list
    book: np.ndarray
    T: int
    dt: float
    ticksize: int = 5

    def __init__(self, world, n, T, dt):
        vals = list(vars(world).values())[1:]
        self.book = np.empty((len(vals), n), dtype=object)    #Create logbook
        self.book[:,0] = vals
        self.att = list(vars(world).keys())[1:]
        self.T = T
        self.dt = dt

    def write(self, world):
        data = list(vars(world).values())
        self.book[:, int(data[0])] = data[1:]                 #Update logbook

    def read(self, cols, first = True):
        if first:
            chapter = self.book[:, :cols]
        elif not first:
            chapter = self.book[:, cols:]
        else:
            print("what do you want to print?")
        print(np.concatenate((np.array(self.att).reshape(-1,1), chapter), axis
    = 1))

    def get(self, var):                                      #Get one variable
        try:
            return self.book[self.att.index(var)]
        except:
            print(var, 'is not an attribute of this instance of Log')
```

C.4 Behaviour model

```python
#backward Euler and kappa separate with interpolation - version for two-way
    coupling

import numpy as np
import copy
import matplotlib.pyplot as plt
import scipy

#the -1 indicates the value of the previous timestep
def mitigator_step(x1, kappa1, kappa, Lambda1, Lambda, Omega1, Omega,
                                                    delta1, delta, dt):

    #implicit function to solve
    def x_impl(x, dt, kappa, x1, Lambda, Omega, delta):
        return x-x1-kappa*dt*x*(1-x)*(-Lambda + Omega + delta*(2*x-1))

    #interpolate the step when needed
    def intp(dt, kappa1, kappa, Lambda1, Lambda, Omega1, Omega, delta1, delta):
        kappai = 0.5*(kappa1 + kappa)
        Lambdai = 0.5*(Lambda + Lambda1)
        Omegai = 0.5*(Omega + Omega1)
        deltai = 0.5*(delta + delta1)
        return dt/2, kappai, Lambdai, Omegai, deltai

    #perform a timestep
    def backward(dt, x1, kappa1, kappa, Lambda1, Lambda, Omega1, Omega,
                                                        delta1, delta):
        func    = lambda y: x_impl(y, dt, kappa, x1, Lambda, Omega, delta)
        #Forward Euler as guess for rootfinding
        x_fe = x1 + kappa1*dt*x1*(1-x1)*(-Lambda1+Omega1+delta1*(2*x1-1))
        result  = scipy.optimize.root(func, x_fe, method="hybr")
        #print(x_fe, result.x)

        #when no success use interpolation
        if not result.success:
            #print("root finding failed", "found x = ", result.x[0])
            dti, kappai, Lambdai, Omegai, deltai = intp(dt, kappa1, kappa,
                                Lambda1, Lambda, Omega1, Omega, delta1, delta)

```

```
            xi, ti    = backward(dti, x1, kappa1, kappai, Lambda1, Lambdai,
                                            Omega1, Omegai, delta1, deltai)
            xi_2, ti_2 = backward(dti, xi[-1], kappai, kappa, Lambdai, Lambda,
                                            Omegai, Omega, deltai, delta)
            return np.append(xi, xi_2), np.append(ti, ti_2+ti[-1])

        #for negative root choose a different root
        if result.x[0]<0.:
            print('found negative root')
            roots = np.array([])
            for guess in np.linspace(-1, 1, 100)[::-1]:
                r = scipy.optimize.root(func, guess, method="hybr")
                if r.success:
                    roots = np.append(roots, r.x[0])
            roots = np.round(roots, decimals=5)
            print('The roots are: ', set(roots))

            roots_pos = roots[np.where(roots>0.)]
            if len(roots_pos) == 1:
                new = roots_pos[0]
            elif len(roots_pos)>1:
                new = min(roots_pos, key = lambda y: abs(y-x1))
            else:
                new = max(roots)
            result = scipy.optimize.root(func, new, method="hybr")
            print('choose root ', result.x)
        return result.x, np.array([dt])

    xi, ti = backward(dt, x1, kappa1, kappa, Lambda1, Lambda,
                                Omega1, Omega, delta1, delta)
    return xi, ti
```

C.5 Coupled model

```
from DICE2023_implementatie_v11 import *
from DICE2023_fastsystemv2 import *
from Behaviour_modelv12 import *
import math
import random
```

```

#Default parameters for the coupling
@dataclass
class Beh_par():
    low:    float = 0.0
    high:   float = 0.04
    nu1:    float = 18.33823795121729
    nu2:    float = 320.4820049354229

nu1     = 18.33823795121729     #2./max value of theta1
nu2     = 320.4820049354229     #f(1.5)/Omega(1.5)

#functions to couple social model to DICE
def x_to_dmu(x, low, high):
    return (1-x)*low+x*high

def mu_step(mu1, dt, dmu):
    new_mu = mu1 + dt*dmu
    if new_mu > 1.:
        return 1.
    if new_mu < 0.:
        return 0.
    return new_mu

#perform a timestep of the coupled model
def timestep(dt, s1, p, x, kappa1, kappa, delta1, delta, mu1, mu, p_b):
    s       = s1.timestep(p, dt, mu1, mu)
    xi, ti  = mitigator_step(x, kappa1, kappa, p_b.nu1*s1.Lambda,
                    p_b.nu1*s.Lambda, p_b.nu2*s1.Omega, p_b.nu2*s.Omega,
                    delta1, delta, dt)
    dmu     = x_to_dmu(xi[-1], p_b.low, p_b.high)
    mu_next     = mu_step(mu, dt, dmu)
    return s, xi[-1], mu_next

#run the coupled model
def coupled(n, dt, T, x0, mu0, kap, delt, p_b):
    p, s    = initialize(n, dt)
    s.mu    = mu0
    log     = Log(s, n, T, dt)
```

```
    kappa    = kap
    kappa1   = kap
    delta    = delt
    delta1   = delt
    x        = np.empty(n)
    x[0]     = x0
    x[-1]    = x0
    mu       = np.empty(n+1)
    mu[0]    = mu0
    dmu0     = x_to_dmu(x[0], p_b.low, p_b.high)
    mu[1]    = mu_step(mu[0], dt, dmu0)
    for i in range(1, n):
        s, xi, mu_next   = timestep(dt, s, p, x[i-1], kappa1, kappa,
                                    delta1, delta, mu[i-1], mu[i], p_b)
        log.write(s)
        x[i]             = xi
        mu[i+1]          = mu_next
    return log, x, mu, s

def eq_2t(log, par, mu, dt, tau0):
    i_2t     = int(tau0/dt)
    eq       = World()
    eq.R0    = log.get('R0')[i_2t]
    eq.R1    = log.get('R1')[i_2t]
    eq.R2    = 0.
    eq.R3    = 0.
    eq.T1    = log.get('T1')[i_2t]
    eq.M_AT = eq.R0 + eq.R1 + par.M_AT0
    eq.C_acc = log.get('C_tot')[i_2t] - (eq.M_AT - par.M_AT0)
    eq.F     = par.F_EXlim + par.eta**np.log(eq.M_AT/par.M_AT0)/np.log(2)
    eq.T2    = 0.44*eq.F
    eq.T_AT = eq.T1 + eq.T2
    eq.maxT_AT   = np.max(log.get('T_AT'))
    def alpha_2t(alpha, par, eq):
        val = -(par.zeta[0]+par.zeta[1]*eq.C_acc + par.zeta[2]*eq.T_AT)
                                                + alpha*par.xi[3]*par.tau[3]
        for i in range(3):
            val += alpha*par.xi[i]*par.tau[i]
```

```
                                                        *(1-np.exp(-100/(alpha*par.tau[i])))
            return val

    fun       = lambda x: alpha_2t(x, par, eq)
    result    = scipy.optimize.root(fun, log.get('alpha')[i_2t], method="hybr")
    if not result.success:
        print('alpha not found for finding equilibrium')
    eq.alpha = result.x[0]
    return eq
```

C.6 Example main code

```
#Main code coupled model
from Coupled_modelv4 import *
plt.rcParams['axes.titlesize'] = 14
plt.rcParams['axes.labelsize'] = 12

T        = 3005
dt       = 5
n        = int(T/dt)
tau0     = 3000
x0       = 0.05#0.0001
mu0      = 0.05
kappa1   = 0.2
kappa    = 0.2
delta    = 2.
delta1   = 2.

low      = 0.0
high     = 0.04
nu1      = 18.33823795121729      #2./max value of theta1
nu2      = 320.4820049354229      #f(1.5)/Omega(1.5)
p_b      = Beh_par()

log, x, mu, s    = coupled(n, dt, T, x0, mu0, kappa, delta, p_b)

time = np.arange(0, T, dt)
plt.plot(time, log.get('T_AT'))
plt.xlabel('t [y]')
```

```
plt.ylabel('$T_{AT}$ [$^\circ$C]')
plt.show()

#Main code DICE
from DICE2023_implementatie_v11 import *
from DICE2023_fastsystemv2 import *

T = 3005
dt = 5
n = int(T/dt)

p, step = initialize(n, dt)
p.mu = mu_tanh(n, dt, T_mu)
log = Log(step, n, Tr, dt)
for _ in range(n-1):
    step = World.timestep(step, p, dt)
    log.write(step)
eq   = Eco_eq2t(step, p)
print('Equilibrium temperature = '+str(eq.T_AT))

plt.plot(np.arange(0, n*dt, dt), log.get("T_AT"))
plt.xlabel("$t$ [y]")
plt.ylabel("$T_{AT}$ [$^\circ$C]")
plt.show()
```